International Geology Review

ISSN: (Print) (Online) Journal homepage: www.tandfonline.com/journals/tigr20

Large Fe-Mn oncoids from Early Jurassic Ammonitico Rosso Facies (eastern Sakarya Zone, NE Turkey): new insight into palaeogeographic conditions of Tethys Ocean

Raif Kandemir, Merve Özyurt, Yılmaz Demir & Orhan Karsli

INTERNATIONAL GEOLOGY REVIEW
https://doi.org/10.1080/00206814.2024.2364367

Taylor & Francis
Taylor & Francis Group

Large Fe-Mn oncoids from Early Jurassic Ammonitico Rosso Facies (eastern Sakarya Zone, NE Turkey): new insight into palaeogeographic conditions of Tethys Ocean

Raif Kandemir[a,b], Merve Özyurt[b], Yılmaz Demir[a] and Orhan Karsli[b]

[a]Department of Geological Engineering, Recep Tayyip Erdoğan University, Fener-Rize, Turkey; [b]Department of Geological Engineering, Karadeniz Technical University, Ortahisar-Trabzon, Turkey

ABSTRACT

Oncoids, significant sedimentary structures within the Jurassic strata of the Mediterranean Region, serve as valuable indicators of paleoenvironmental conditions during their formation. One of the important examples of oncoids has been discovered in the Pliensbachian (Early Jurassic) Ammonitico Rosso Facies (ARF) of the eastern Sakarya Zone (Eastern Pontides, NE Turkey). This study presents the first comprehensive sedimentological and petrographic (textural and compositional characteristics) examination, as well as geochemical analyses (trace and rare earth elements) of these Fe-Mn oncoids. The oncoids consist of nuclei coated with irregular laminae and exhibit a range of sizes, from 10 to over 45 mm, displaying various colours such as brown, reddish, and metallic-looking. They mostly have a discoidal shape, although some are spherical. The nuclei consist of bioclastic wackestones, containing remnants of ammonoid shells. Some oncoids, especially the discoidal forms, have multiple nuclei. The cortex of the oncoid predominantly consists of wrinkled bands displaying micritic laminae, with an abundance of filamentous bodies and the local presence of encrusting microfossils. In the cortex of the oncoids, iron predominates over manganese, and there are compositional variations within the cortex, especially enriched in Si, Fe, and Ca. They predominantly fall within the region associated with hydrothermal Fe and Mn sediments, as indicated by discrimination diagrams involving Ni, Co, Zn, and plots of Ce/Ce* vs Y/HoN and Nd contents, suggesting a hydrothermal origin. Furthermore, their rare earth elements (REE) chemistry displays distinct Y/Ho, Sm/Yb, Ce/Ce, and Nd values, indicating the presence of seawater mixing with hydrothermal fluids. However, they show relatively low Sm/Yb, Y/Ho, Eu/Sm, Nd/YbN, and La/Yb values, suggesting a limited contribution from hydrothermal sources to the surrounding seawater. Nevertheless, the cortex of the oncoids exhibits a complex and variable mineralogy that changes over short distances, implying the dynamic nature of the depositional environment, characterized by fluctuating hydrological regimes, varying oxygen levels, elemental supply, and the saturation of specific elements in seawater. The increased presence of specific trace elements, including Fe, and REE during this period, is likely linked to hydrothermal fluid input into marine environments, coinciding with intensified syn-sedimentary tectonic activity, where ongoing extensional tectonic movements occasionally influenced paleoenvironmental conditions. In these conditions, the formation of oncoids is influenced by various sedimentary factors, including the availability of metal sources, specific paleoenvironmental conditions, and the presence of microbial organisms, thereby enriching our understanding of palaeogeography during the Early Jurassic period. Additionally, the studied oncoids, with their comparable stratigraphic position and petrographic characteristics to those in both the eastern and western parts of the Tethyan basin, underscore their significance in palaeogeography and stratigraphy.

ARTICLE HISTORY
Received 8 January 2024
Accepted 2 June 2024

KEYWORDS
Fe-Mn oncoid; amonitico rosso; late triassic to early jurassic; REE; eastern Sakarya Zone

1. Introduction

Oncoids are distinctive bio-sedimentary structures that are mostly characterized by spherical nodules composed of concentric laminae enveloping a biogenic or abiogenic nucleus (Tucker and Wright 1990; Flügel 2012). Flügel (2012) defines oncoids as unattached, rounded nodules ranging from millimetres to centimetres in size, composed of either calcareous or non-calcareous nodules. Non-carbonate oncoids encompass phosphatic, ferruginous, and manganese nodules (Flügel, 2004; Flügel 2012), with less frequent occurrences of oncoids composed of pyrite (Schieber 1999) or chlorite (Misik and Sucha 1997). Among the various types of oncoids, Fe-Mn macro-oncoids stand out as sedimentary

CONTACT Merve Özyurt merveyildiz@ktu.edu.tr Department of Geological Engineering, Karadeniz Technical University, Ortahisar-Trabzon 61080, Turkey
Supplemental data for this article can be accessed online at https://doi.org/10.1080/00206814.2024.2364367

structures containing significant amounts of iron (Fe) and manganese (Mn) minerals (e.g. Jones and Renaut 1997a, 1997b; Pérez and Nieto 2010; Zang *et al*. 2015; Reolid and Abad 2019). Fe-Mn macro-oncoids have been documented in various geological settings, including marine environments and other depositional settings (e.g. Jenkyns 1970; Tucker and Wright 1990; Preat *et al*. 2000; Reolid and Nieto 2010). They are notably prevalent throughout the Mesozoic Tethyan region within condensed pelagic limestones (Jenkyns 1970; Jones and Renaut 1997a, 1997b; Pérez and Nieto 2010; Flügel 2004; Zang *et al*. 2015; Reolid and Abad 2019). According to Flügel (2012), these oncoids are commonly associated with pelagic carbonates and are often found alongside stromatolitic crusts on discontinuity surfaces. They typically correspond to major stratigraphic gaps linked to eustatic highstand phases. Additionally, the formation and spatial distribution of oncoids are predominantly influenced by palaeoclimatic conditions, distinct paleoenvironmental settings, and fluctuations in sea level (Tucker and Wright 1990; Reolid and Nieto 2010; Zafar *et al*. 2024). Microbes can play a significant role in forming these oncoids, facilitating mineralization and sediment trapping and binding (Monty 1984; Flügel 2012). Factors such as the availability of dissolved Fe and Mn in the water column, microbial activity, and physicochemical conditions influence the formation process (Lazăr *et al*. 2013; Reolid and Abad 2019). Oxygen-depleted or reducing environments can be particularly favourable for microbial-mediated mineral precipitation, providing an environment conducive to the development of Fe-Mn macro-oncoids (e.g. Preat *et al*. 2000).

Due to their intriguing features and potential to offer valuable insights into past environmental conditions (such as hydrodynamic regimes, paleobathymetry), palaeogeographic settings, microbiotas, and seawater chemistry, Fe-Mn macro-oncoids have been the subject of extensive research (Jenkyns 1970; Tucker and Wright 1990; Preat *et al*. 2000, 2011; Gradzinski *et al*. 2004; Hägele *et al*. 2006; Sequero *et al*. 2020; Xiao *et al*. 2020; Zafar *et al*. 2024). Although, the investigation into the distribution patterns of marine oncoids garners considerable attention due to their utility in unravelling pivotal sedimentary factors influencing their formation within the distinct geologic setting (e.g. Tucker and Wright 1990; Preat *et al*. 2000; Reolid and Nieto 2010). Despite their profound scientific significance, the origin of oncoids has remained a subject of debate for over a century, primarily due to the intricate array of formation mechanisms involved, Fe and Mn source (Tucker and Wright 1990; Gradzinski *et al*. 2004; Hägele *et al*. 2006; Reolid and Abad 2019).

Important examples of Fe-Mn oncoids are located in the Gümüşhane area (Kandemir and Yılmaz 2009). These Fe-Mn oncoids are found within the Jurassic ARF strata, which is well-dated as the Pliensbachian age (Kandemir and Yılmaz 2009). However, most of these studies focused mainly on the lithostratigraphy and biostratigraphy of Jurassic ARF strata in this region of the eastern Sakarya Zone. However, detailed petrographical and sedimentological investigations, integrated with chemical data, are still lacking, and the genesis of these oncoids remains debate. Therefore, we here present a comprehensive analysis of the sedimentology, microfacies, and distribution of REE characteristics of the oncoids. We also discuss the genesis of microbial oncoids and their association with low deposition rates and controlling factors for their morphology and growth within the context of basin evolution.

2. Geological setting

The study area is situated in the eastern part of the Pontides tectonic unit, within the Gümüşhane region of NE Turkey (Figure 1(a,b)). The Pontides form a mountain range that extends in an east-west direction, located between the Black Sea to the north and the İzmir-Ankara-Erzincan suture to the south (Figure 1(a)). Specifically, the Eastern Pontides refers to the eastern section of the Pontides mountain chain, which corresponds to the Sakarya Zone and represents one of the most well-preserved fossil magmatic arcs (Figure 1(a,b)).

Heterogeneous pre-Jurassic basement rocks of the eastern Sakarya Zone comprises (1) Variscan metamorphic rocks (Topuz *et al*. 2004), (2) Late Carboniferous granitic rocks (Topuz *et al*. 2010), (3) Upper Carboniferous-Lower Permian shallow-marine to terrigenous sedimentary rocks (Okay and Leven 1996; Çapkınoğlu 2003; Kandemir and Lerosey-Aubril 2011) and (4) Permo-Triassic metabasalt-phyllite-marble (Okay 1984).

The Lower-Middle Jurassic volcano-sedimentary sequence is unconformably deposited over heterogeneous Hercynian basement rocks (Vörös and Kandemir 2011). This sequence exhibits significant vertical and lateral variations in facies characteristics and has a variable thickness ranging from 2 to 2243 metres along the basin. It represents a transgressive succession that was deposited during the Hettangian/Sinemurian-Bathonian stages (Figure 2). The sequence comprises conglomerates, sandstones, calcareous and marly Ammonitico Rosso type sediments, as well as volcaniclastic and volcanic rocks. The sandstone unit, which forms the base level of the formation, is overlain by Ammonitico Rosso

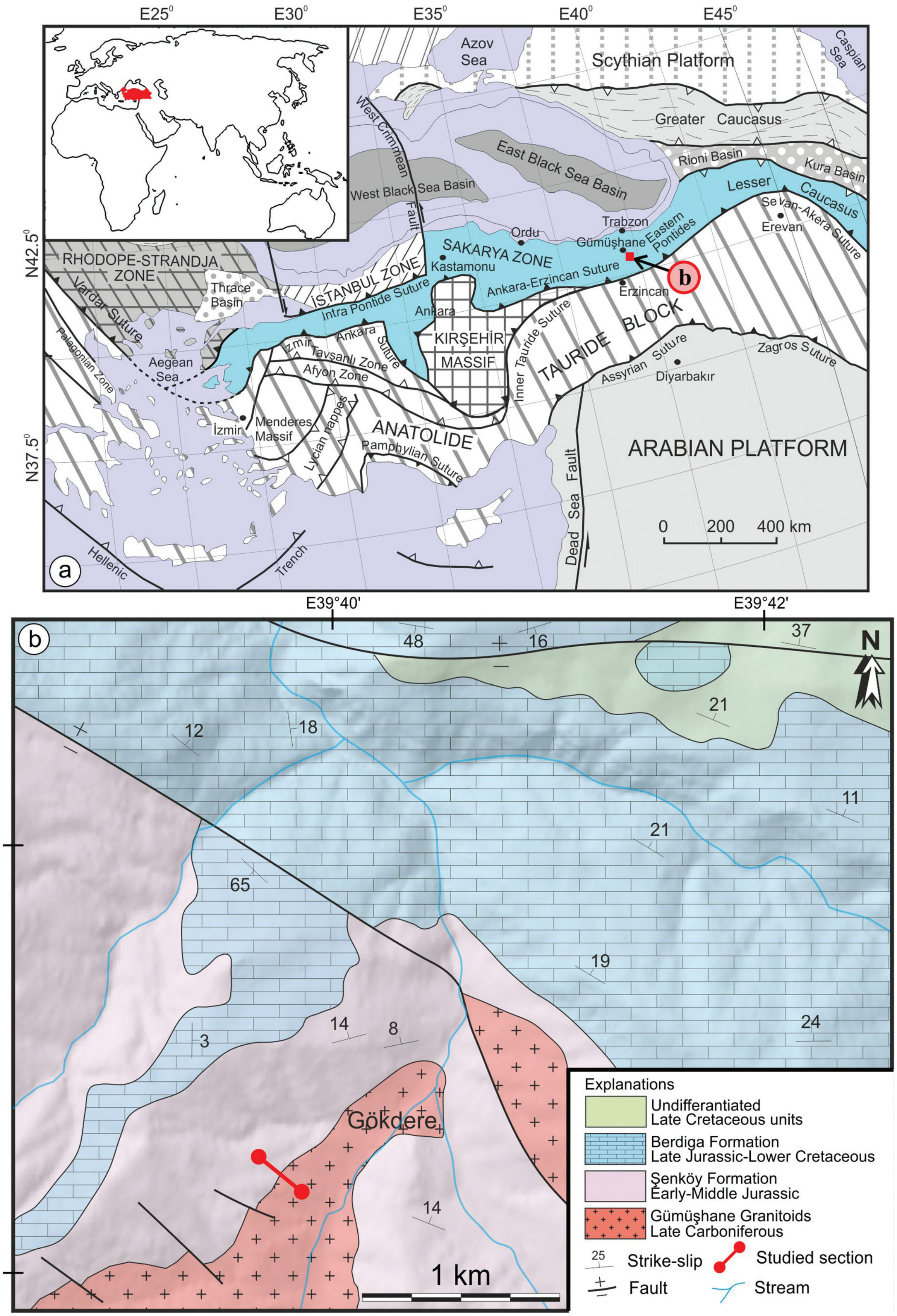

Figure 1. a: Major tectonic units of Turkey (Okay and Tüysüz 1999) and location of the studied area, b: Detailed geological map of the Gökdere area (modified from Kandemir 2004).

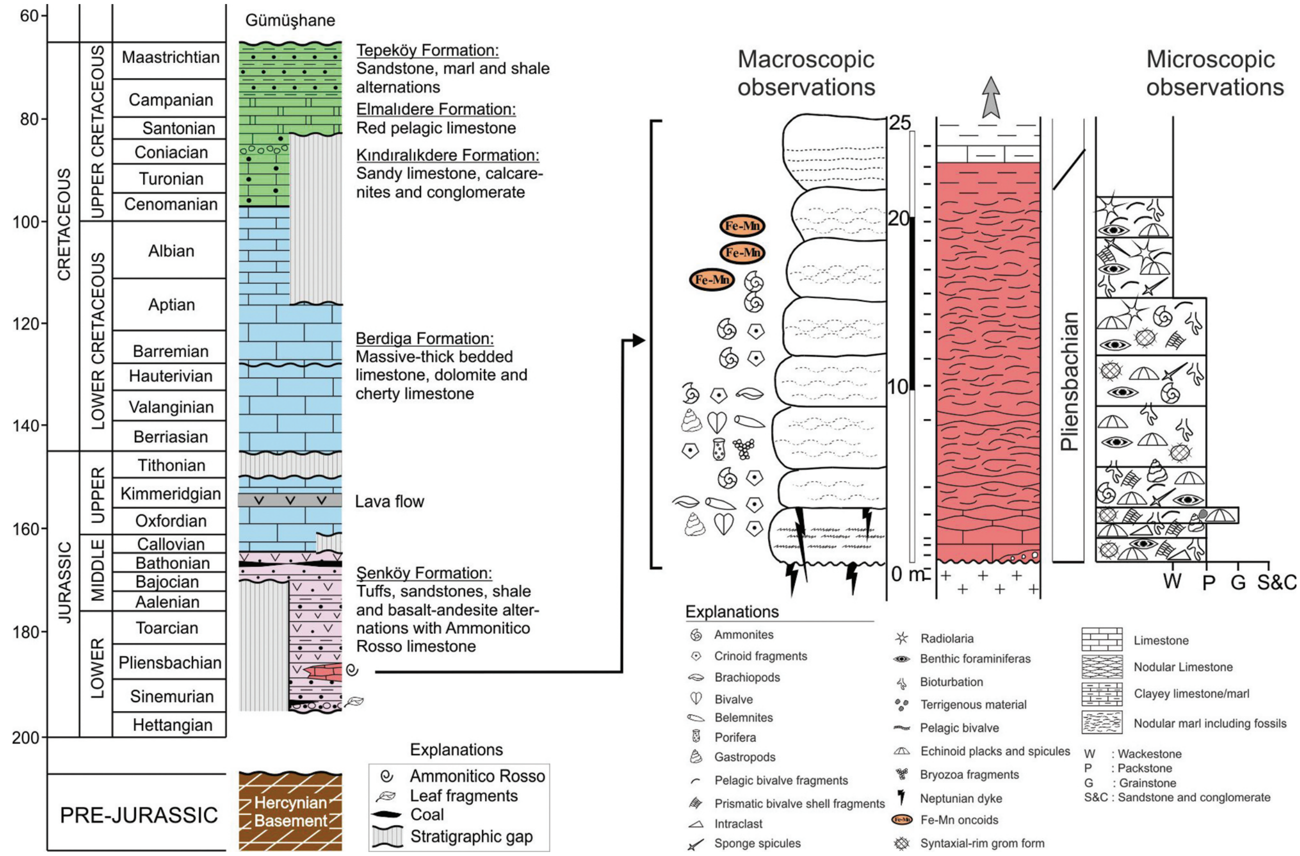

Figure 2. Detailed stratigraphic section of Gümüşhane region and ARF strata in Gökdere area (modified from Kandemir and Yılmaz 2009; Akkemik et al. 2022).

horizons. The age of the Ammonitico Rosso horizons is inferred to be Pliensbachian based on the fossil assemblages, including *Agerina martana* Farinacci, *Involutina liassica* Jones, *Lenticulina* sp., *Frondicularia* sp., *Nodosaria* sp., *Agerina martana*, and *Involutina liassica* (Kandemir and Yılmaz 2009). The Şenköy Formation is conformably overlaid by Upper Jurassic to Lower Cretaceous platform carbonates known as the Berdiga Formation. Benthic foraminiferal assemblages suggest an Oxfordian to Albian age for the platform carbonates in the Eastern Pontides (Pelin 1977; Kırmacı *et al*. 1996; Özyurt et al. 2020, 2022). The succession is further overlain by an Upper Cretaceous unit consisting of yellowish-coloured sandy limestones, red pelagic limestones containing globotruncanids, and locally interbedded siliciclastics with felsic tuff (Pelin 1977; Özyurt *et al*. 2023). The Hercynian basement and post-Hercynian volcano-sedimentary associations have been intruded by Eocene granitic rocks and are unconformably overlain by the Early Cenozoic volcano-sedimentary sequence (Karsli *et al*. 2010) (Figure 2).

3. Materials and methods

The Gümüşhane area of the Eastern Pontides hosts exemplary ARF strata and Fe-Mn oncoids (Figures 1(b) and (2)). The most prominent outcrops of oncoid-bearing strata are located in the Gökdere stratigraphic section (Figure 2). The section was thoroughly examined based on field observations and microfacies properties, as outlined in Kandemir and Yılmaz (2009). This stratigraphic section measured 22 metres, and the most representative 20 samples were collected from the Ammonitico Rosso Formation (ARF) at stratigraphic intervals ranging from 30 to 100 cm. Additionally, 40 oncoid samples were collected from the upper levels of the studied section. 40 thin sections and 13 polished sections of the host rock and the Fe-Mn oncoids were prepared for petrographical analyses. For thin section preparation, the samples were initially cut into 2 × 3 cm dimensions. The sample surface was then smoothed using abrasive powders of varying sizes and affixed to glass using epoxy. The sample surface was gradually abraded with powders of different sizes until reaching a thickness of 30 microns. Thin sections were scrutinized under an Olympus BX51 bottom-illuminated research microscope at Recep Tayyip Erdoğan University. For polished section preparation, samples were placed in a mould with a one-inch diameter and encased in epoxy. The sample surface was abraded using abrasive powders of different sizes to remove roughness gradually. Finally, the surface was polished using aluminium oxide powder. The polished samples were examined under an Olympus BX51top-illuminated research microscope at Recep Tayyip Erdoğan University. Analysis of the Fe-Mn oncoids, encompassing the characterization of cortical structure, nucleus, and coat thickness, was performed on the most representative oncoid samples. The mineral composition of the Fe-Mn crusts and coated grains was determined using X-ray diffractometry (XRD-RigakuSmartLab) and scanning electron microscopy (SEM-JeolJSM-6610) with back-scattered electron (BSE) imaging analysis. To ensure sample conductivity, all samples were initially coated with 99% pure gold (Au) using a coating device (Quorum brand, model SC-7620) in argon gas for 150 seconds, resulting in a coating thickness of approximately 200 angstroms. The surface morphology of the coated samples was examined using a scanning electron microscope (JEOL brand, JSM 6610 model) with an accelerating voltage of 15 kV under vacuum. Compositional analysis and elemental mapping were determined using energy dispersive X-ray spectroscopy (EDS) coupled with SEM (Oxford Instruments, Inca X-act). For the trace element analyses, the most representative thin sections and mirror-image slabs of each thin section were meticulously polished to assess weathering and micro-fractures filled with calcite or clastic components, ensuring their exclusion during geochemical sampling. The cortex of oncoids in each polished slab was sampled using a hand drill with micro-drilling techniques. Additionally, micritic orthochemical carbonate particles from the host rocks of each polished slab were sampled using a hand drill with micro-drilling techniques for trace element analyses.

Additionally, the trace element composition of six samples, three from oncoids and the remaining from the host sediment, was analysed using an inductively coupled plasma-mass spectrometer (ICP-MS) at ACME laboratory in Canada. To ensure precision and accuracy, 1 mL of an internal standard containing Bi, Sc, and In was added to the solution. For detailed information on these methods, please refer to the website http://acmelab.com. The detection limits for Ba, Ni, and Sc are 1, 20, and 1 ppm, respectively. Additionally, for Hf, Zr, Y, La, and Ce, the detection limits are 0.1 ppm, while for Th and Nd, they are 0.2 and 0.3 ppm, respectively. The detection limits for Tm, Tb, and Lu are 0.01 ppm; for Pr, Eu, and Hu, they are 0.02 ppm; for Er, it is 0.03 ppm; and for Sm, Gd, Dy, and Yb, they are 0.05 ppm. Additionally, [$CeN/CeN* = CeN/(0.5LaN + 0.5PrN)$; $EuN/EuN* = EuN/[(SmN \times 0.67) + (TbN \times 0.33)]$, where N refers to normalization to post-Archaean Australian Shale (PAAS-normalized value) (Taylor and McLennan 1985). These equations are used to express Eu and Ce anomalies in the studied samples (Bau and Dulski 1996; Shields and Stille 2001).

4. Results

4.1. Stratigraphy and sedimentology

The Gümüşhane region, from which our oncoids were collected, is known for its Early Jurassic carbonates referred to as ARF (Kandemir and Yılmaz 2009). These ARF are found in the lower portion of the Şenköy Formation, which is preserved in the Gümüşhane region (Kandemir 2004). The ARF passes upward to volcanic and volcaniclastic rocks, including volcanogenic sandstones, siltstones, tuffites, tuffs, pillow lava basalts, shales, and turbiditic sandstones. The ARF strata contain ammonites, brachiopods, bivalves, gastropods, belemnites, crinoids, and foraminiferas (Figure 2). Based on the benthic foraminiferal fauna, the age of the ARF is inferred to be Pliensbachian by Kandemir and Yılmaz (2009). This age is supported by the presence of four species of ammonites in the Gümüşhane-Bayburt regions (Alkaya and Meister 1995). According to fossil determinations, the ARF is dated as Pliensbachian (Kandemir and Yılmaz 2009). The ARF in the Gümüşhane and Gökdere area can be classified into two major types: (a) nodular calcareous ARF and (b) marly ARF (Figure 2) (Kandemir and Yılmaz 2009). These types differ from each other in terms of their structural and textural properties. Microbially-formed Fe-Mn oncoids have been observed in the marly ARF strata (Figure 2).

The marly ARF exhibit a distinct nodular appearance in outcrop due to the differential weathering of the red-brown nodules and the brick-red, clay-rich matrix (Figure 3(a-d)), distinguishing them from the nodular calcareous ARF strata. The marly ARF strata mainly consists of wackestone and is particularly rich in ammonites and belemnites. In the Gökdere section, the upper level of the facies contains microbially-formed Fe-Mn oncoids associated with ammonites (Figures (2) and 3(e-f)). The investigated oncoids were previously interpreted as nodules (Kandemir 2004; Kandemir and Yılmaz 2009) but are now identified as oncoids for the first time in this study.

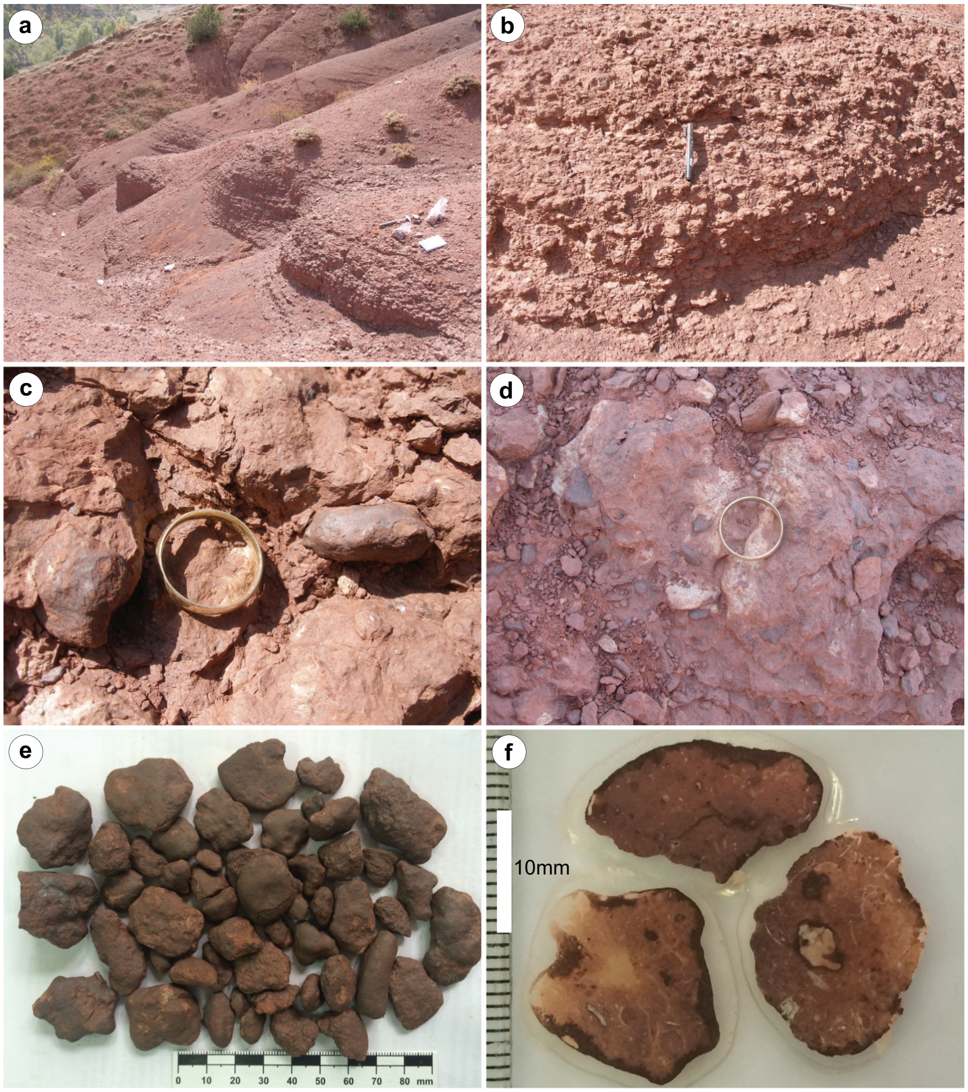

Figure 3. a: Field view of the marly ARF strata in Gökdere, b: Close view of the marly ARF strata and nodules, c and d: Close view of the Fe-Mn oncoids in host sediments (diameter of the ring is 2 cm), e: Oncoids in Gökdere section, f: Cross-section of some oncoids (scale bar is mm).

4.2. Morphology and structure of oncoids

The oncoids range in size from 10 to 45 mm across (Figures 3(b-d), 4(a-j), 5a). They exhibit brown, reddish, and metallic colours (Figure 3(e,f)). Most of the oncoids are discoidal in shape, with some also spherical. The oncoids consist of nuclei coated with irregular laminae (Figures 3(f) and 4(a-c)). The nuclei comprise bioclastic wackestones, which contain ammonoid shells and moulds. These wackestones also contain a similar fossil assemblage, including thin-shelled ostracods, radiolarians, and sponge spicules, akin to their host rocks. Additionally, mollusc shell fragments and benthic foraminifera such as *Involutina* sp., *Lenticulina* sp., *Frondicularia* sp., and *Nodosaria* sp. are also present in their host rocks (Kandemir and Yılmaz 2009). Some oncoids, particularly the discoidal forms, exhibit multiple nuclei (Figure 4(b,c)). Additionally, Fe-Mn-coated echinoid fragments and spines, as well as micro borings filled with Fe-Mn oxides, can be observed (Figure 4(e,f)). The macro oncoids, with an average size of 35 mm, consist of microbial laminae that exhibit rhythmic growth (Figure 4(g-j)). The cortices of the oncoids predominantly consist of wrinkled bands and are composed of dark-red laminae, encrusting fossils (Figure 4(a-j)). The macro oncoids, with an average size of 35 mm, consist of microbial laminae that exhibit rhythmic growth (Figure 4(g-j)). The coating thickness is less than 2 mm, and the shapes display an arborescent to dendritic microstructure. Laminae exhibit irregular, random growth and can also produce microscale-lobate growth forms resembling Type L as defined by Flügel (2004) (Figure 5(a)). Additionally, some parts of

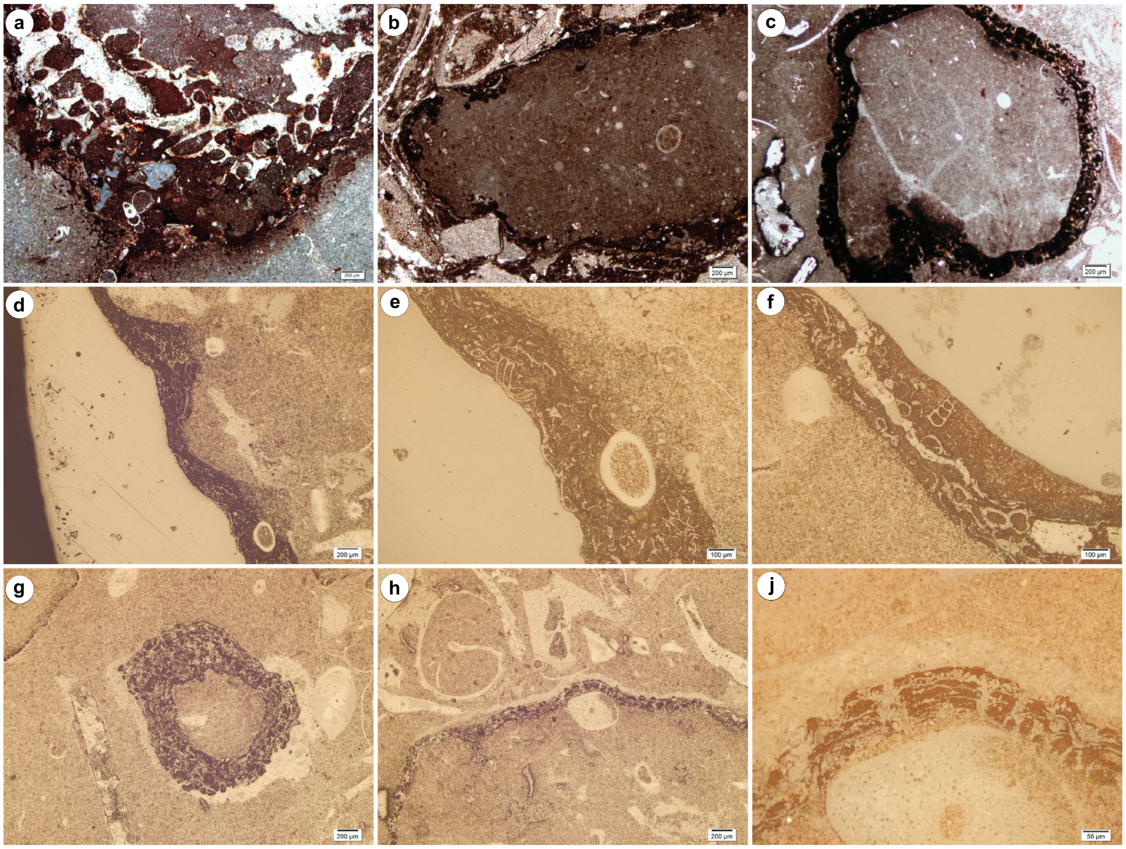

Figure 4. Thin sections (a to c) and polished sections (d to j) of cortex and nuclei of oncoids.

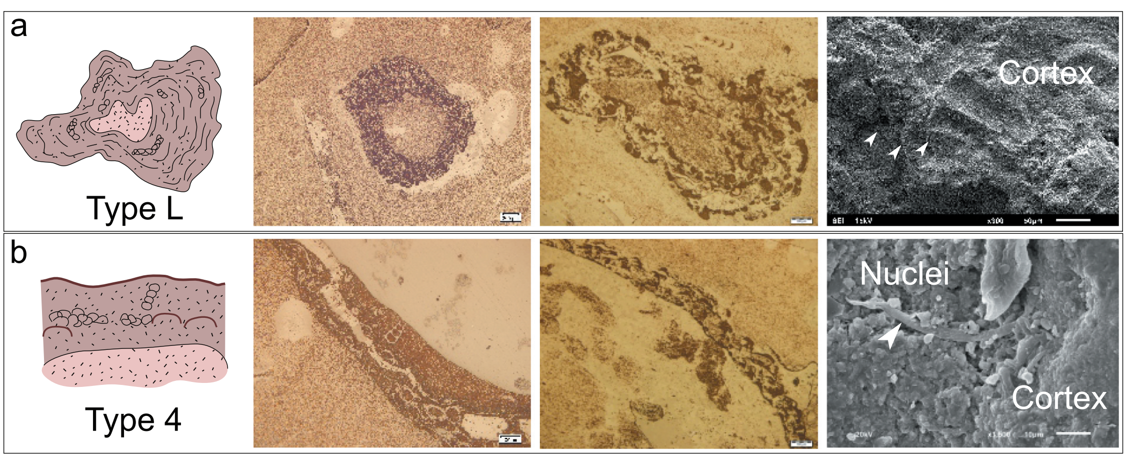

Figure 5. a: Geometric types of oncoids, views of the sections, and SEM images (white arrows indicate different layers of the cortex). b: Types of laminae, including micritic laminae alternating with layers of recognizable encrusting microfossils, along with views of the sections and SEM images (white arrows indicate encrusting organisms) (Flügel 2004).

oncoids consist of micritic material, with laminae including or alternating with layers of recognizable encrusting microfossils resembling Type 4 as defined by Flügel (2004) (Figure 5(b)). Although the specific genera of the encrusting fossil are undetermined, they are also observed in arborescent morphologies on the coating. Various encrusting organisms have been found on the cortices' surfaces and between specific laminae, with Serpulids? dominating in certain sections (Figure 5(b)). The coating ranges from 20 to 200 μm thick, forming densely packed accumulations mainly consisting of Serpulids? Aggregates. Additionally, this type of oncoid lacks well-defined

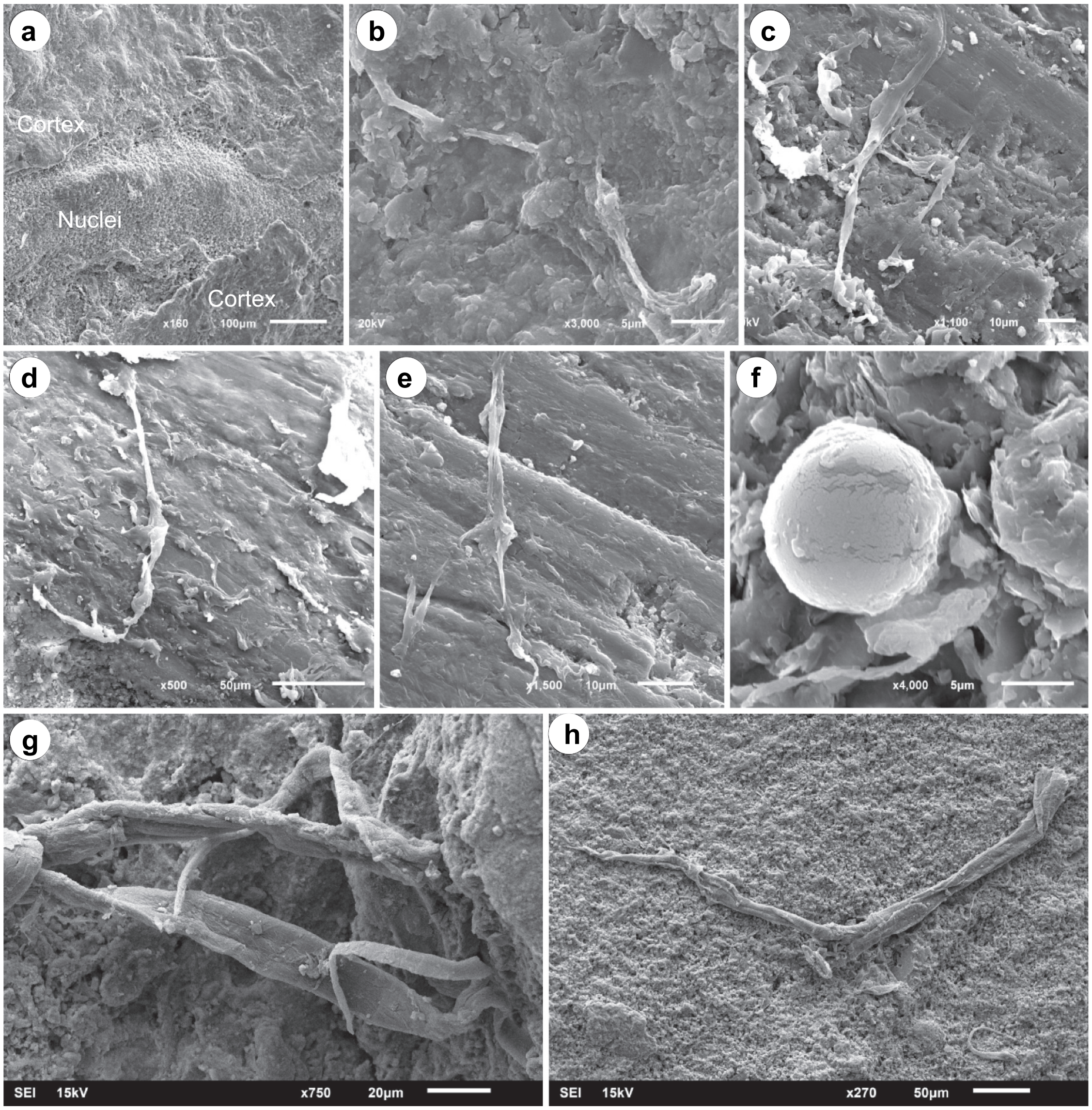

Figure 6. a: SEM images of the cortex and nuclei from the surface of oncoids. b: SEM images showing microbial structures observed inside Fe-Mn oncoids. c-d-e: SEM images displaying filamentous structures observed on the surface of the Fe-Mn oncoids. f: Probable fungal spore or goethite microspherules observed in the cortex of an oncoid. g-h: SEM images showing filamentous and web-like structures observed on the surface of the Fe-Mn oncoid cortex.

lamination or the meshwork characterizing other types (Figure 5(b)) which are well-conforming with Type 4 (Flügel 2004). Segmented filaments can be observed on the cortices of the oncoids through SEM analysis, allowing for the identification of filament webs with a cylindrical shape (Figure 6(a-f)). These structures closely resemble fungal hyphae by their shape.

4.3. Chemical and mineralogical composition of oncoids

The oncoid cortices are predominantly composed of hematite and manganite, as revealed by XRD analysis (Supplementary Figure S1). The core of the oncoid is represented by Ca-bearing minerals. The cortex of the studied oncoids is characterized by complex and variable mineralogy that changes over short distances. Hematite, manganite, and quartz are the main mineral associations of the mineralized cortex. Different compositional zones (including enrichment in Si, Fe, and Ca, along with another trace element) within the mineralized cortex are also observed. Chemical and EDS analyses, as depicted in Figure 7, have conclusively demonstrated that iron predominates over manganese in the chemical composition of cortex.

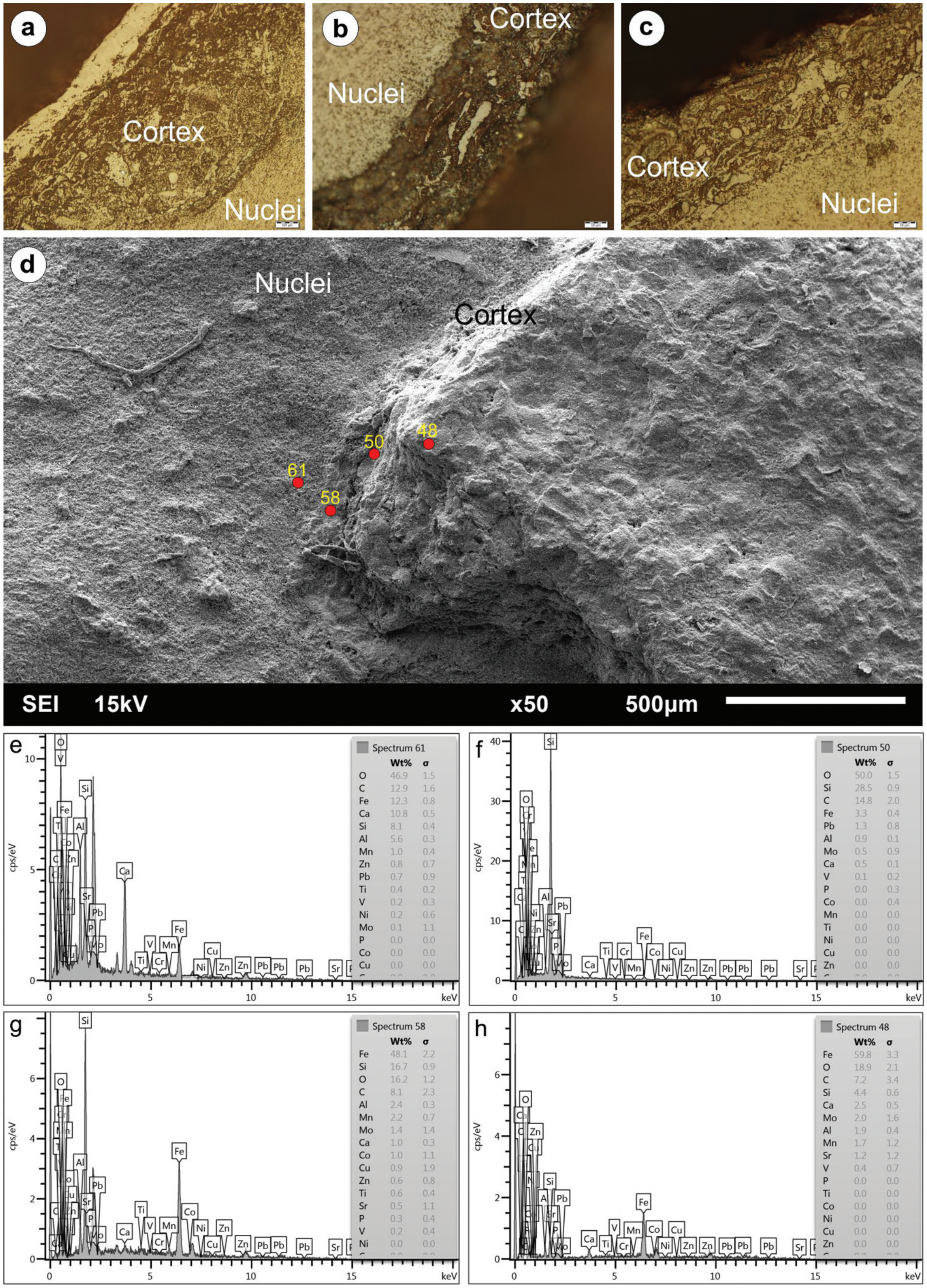

Figure 7. a-c: The view of the cortex on the oncoid nucleus (white arrow shows serpulid? Tube section), d: The SEM view of the cortex and nuclei and selected EDS points to analysis, e-h: EDS analysis from different points of the cortex.

The trace and REE data are presented in Supplementary Table 1. The REE abundances (∑REE) in the samples range from 62.55 to 69.85 ppm (66.44 ppm average), which are higher values compared to the REE concentrations of belemnite samples (0.32 ppm to 0.54 ppm) that were recorded in eastern Sakarya Zone. The average ∑REE contents in the oncoids (61.46 ppm) are significantly lower than those in the Post-Archaean Australian Shale (PAAS) (183 ppm; Taylor and McLennan 1985) and North American Shale Composite (NASC) (173 ppm; Boynton 1984). The La/Yb and Y/Ho ratios of the samples vary between 9.85 and 10.00, with an average of 9.92 and 28.54 and 31.60, with an average of 30.26, respectively. Their host rocks have relatively similar La/Yb (9.42 to 11.36, with an average of 10.30) and Y/Ho ratios (30.24 to 34.69, with an average of 32.04). The normalized REE patterns exhibit light rare earth element (LREE) depletion relative to the heavy rare earth elements (HREEs) (average La/YbN of 0.62 and mean Nd/YbN of 0.82). The oncoid samples show a positive La anomaly (average La*/La of 1.29), positive Eu anomaly (Eu/Eu* ranging from 1.23 to 1.27, with an average of 1.26), and a slightly flattened Ce anomaly (Ce/Ce* ranging from 0.91 to 1.08, with an average of 0.99). Their host rock has distinct PAAS normalized patterns, including Ce/Ce* (average 1.12), Eu/Eu* (average 1.27), La/La* (average 1.18), La/YbN (0.70) and Nd/YbN (0.79).

The oncoid samples have relatively high redox-sensitive trace elements including Mo (0.70 to 0.90, average of 0.77), Cu (6.80 to 8.70, average of 8.03), Ni (15.20 to 17.40, with an average of 16.63), and Zn (20.00 to 22.00; ave. 21.00) compared to RSE of limestone samples that recorded in Eastern Pontides (Özyurt *et al*. 2020). Their host rocks have varied Mo (0.70 to 0.90, average of 0.77), Cu (3.60 to 5.60, average of 4.80), Ni (12.30 to 19.00, with average of 15.80), and Zn (18.00 to 23.00; with average 20.67).

5. Discussion

5.1. Implications for paleogeographic conditions

The studied Fe-Mn oncoids are discovered in the Early Jurassic red nodular-marly ARF, representing condensed sedimentation in the Gümüşhane region. These nodules exhibit distinct petrographical features, including brown and black colouration, smooth and compact discoidal shapes, and dense structures with diameters ranging from a few millimetres to 5 centimetres. The cortex of the oncoids displays a unique morphology and dimensions (Figure 7(a-c)). Filamentous bodies within the oncoids (Figure 6(a-e)) are likely mineralized bacterial cells, indicating their microbial origin. Gradzinski *et al*. (2004) discussed that the same SEM investigations have revealed the presence of microfilamentous or spongy networks that probably represent fossilized fungal mats, and the concretions are attributed to foraminiferal-fungal macrooncoids at Tatra Mountains, Poland. However, the precise identification of the microbe types is challenging due to the extensive mineralization of the microbial structures (Reolid and Nieto 2010).

Additionally, spherical bodies resembling fungal spores can be observed among the filaments (Figure 6f). However, these spherical objects are also identified as goethite microspherules within the cortex of ooids in ooidal ironstones by Kalinina *et al*. (2024). Segmented filaments resembling fungal hyphae are also present on the oncoid cortices, as observed through scanning electron microscopy (Figure 6(e-h)). The mineralization process is closely associated with the presence of benthic microbial communities (Figure 4(e,f)), including fungal mats and other microbes (Figure 6(e,f)). Furthermore, the studied core of the oncoid exhibits associations with both benthic and planktonic fauna, most of which have mineralized coatings (Figure 4). This suggests that mineralization was controlled by syn-sedimentary processes at the water-sediment interface. The oncoid's irregular coating consists of laminae with varying thicknesses, ranging from millimetres to centimetres (Figures 3(e,f) and 4(d-f)). The coating displays an alternation of light and dark laminae, with minimal encrustation by microfossil (Figure 4(d-f)). The coating also exhibits a fibrillar meshwork, implying the presence of a Microcoleus mat signature. The filamentous microstructures within the oncoids show a wide range of microspheres, indicating trichomonal arrangements (Figure 6(a-f)). These observations are consistent with microboring in macro-oncoids, similar to the Jurassic Oncoid reported by Reolid and Nieto (2010). The petrographic characteristics of the oncoids provide compelling evidence for the synsedimentary consolidation of the microbialite cortex (Reolid and Nieto 2010).

The distinct PAAS-n REE patterns observed in the studied oncoids and their host micritic rocks, characterized by the absence of a noticeable Ce anomaly but a positive Eu anomaly, imply the prevalence of slightly oxygen-deficient conditions during their formation and the deposition of the sedimentary host rocks (Özyurt *et al*. 2023; Özyurt and Kırmacı 2024). The specific foraminifera fossil assemblage found in the host rocks, such as *Lenticulina* sp. (Kandemir 2004) demonstrates adaptation mechanisms for thriving in mildly reducing, oxygen-restricted conditions, thus providing further support for these environmental conditions (Reolid *et al*. 2013). Additionally, an additional fossil resembling Serpulids (?) was also observed in Figure 7(a-c). In environments marked by unusual stress factors, serpulids have emerged as the predominant component of build-ups, as documented by various researchers (Palma and Angeleri 1992; Friebe 1994; Fornós *et al*. 1997; Cirilli *et al*. 1999; among others). This dominance may occur in tandem with low oxygen levels or eutrophic conditions (Reolid and Molina 2010). The identification of bacteria and fungi (Figure 6b-f) in the cortex can further reinforce the presence of dysaerobic conditions. The association of encrusting fossils and microbial films, composed of cyanobacteria and fungi, observed under these conditions could be explained as evidence of a close symbiotic relationship between microbes and fossils, as suggested by Gradzinski *et al*. (2004) for microbial-foraminiferal oncoids during the Toarcian period. Reolid and Nieto (2010) also proposed this type of association for Jurassic Fe-Mn macro-oncoid.

On the other hand, studies focusing on the Jurassic ferruginous oncoliths, which consist of chamosite minerals in subsurface layers, have proposed that chamosite, being unstable in the presence of free oxygen, requires a mildly reducing environment for its formation (Jones 1984; Palmer and Wilson 1990). Therefore, based on our sedimentological and geochemical data from the Early Jurassic oncoids in the Eastern Pontides, it is probable that mildly reducing paleoenvironmental conditions have influenced the oncoid formation (Ghiorse and Ehrlich 1992; Konhauser 1998). However, it is important to note that the mildly oxygen-depleted conditions and element input were likely unstable, as evidenced by the complex and variable mineralogy observed in the cortex of the studied oncoids, which exhibits changes over short distances (Figure 7(d-h)).

Apart from the unstable oxygen level, other palaeogeographic conditions also influence the formation of the oncoids, although the role of paleoenvironmental conditions, including palaeo-depth in oncoid generation, remains a topic of debate (e.g. Preat *et al*. 2000; Gradzinski *et al*. 2004). Defined by Tucker and Wright (1990) as irregularly shaped coated grains exceeding 2 mm in diameter, oncoids are predominantly associated with shallow-water environments, where they are formed by photosynthetic cyanobacteria and algae (Tucker and Wright 1990; Badenas and Aurell 2010; Olivier *et al*. 2011). Nonetheless, oncoids are also documented in deeper-water settings, where they are believed to originate from non-photosynthetic microorganisms such as bacteria and fungi, thriving in dim or light-deprived conditions (Gradzinski *et al*. 2004; Reolid and Nieto 2010; Reolid 2011). Conflicting reports exist regarding the palaeo-depth, with some suggesting shallow water conditions based on the presence of phototrophic organisms (Santantonio 1993). Nevertheless, it should be noted that stromatolites, often used as depth indicators, cannot reliably determine palaeo-depth as Jurassic stromatolites have been documented in deeper marine environments characterized by aphotic conditions (Böhm and Brachert 1993). Additionally, both phototrophic and non-phototrophic organisms can contribute to the development of micro-boring structures (Golubic *et al*. 1984). In the eastern Sakarya Zone, the presence of benthic and planktonic fauna assemblages within the marly wackestone facies, where the oncoids occur, suggests a deepening of the basin (Özyurt *et al*. 2020; Kandemir *et al*. 2022). The core of the studied host rocks contains ammonite shells, most of which show little to no dissolution, indicating that the deposition likely did not extend much deeper than the aragonitic lysocline (e.g. Tyszka and Kaminski 1995; Preat *et al*. 2000; Birkenmajer 2001; Jach and Starzec 2003; Gradzinski *et al*. 2004). The presence of endolithic borings in the studied oncoids suggests that they were formed in a depositional environment within the photic zone, where light penetration allowed for the colonization of organisms that create borings.

Additionally, the classical interpretation posits that the rounded shape and concentric laminae of oncoids arise from frequent overturning induced by water turbulence (Tucker and Wright 1990; Hägele *et al*. 2006). Consequently, the petrographic features of the analysed oncoids might indicate paleoenvironmental conditions characterized by mild or intermittent agitation from time to time (Logan *et al*. 1964; Lencina *et al*. 2023). These episodes of relatively higher energy leading to overturning phenomenon could facilitate microbial growth on all sides (Figures 5, 7(a-c), 9(e)). Furthermore, the disturbance of re-working of the sediment on the subsurface of the basin by burrowing organisms may also contribute to the movement of oncoids (Massari and Dieni 1983; Gradzinski *et al*. 2004). Similarly, the oncoids documented by Burkhalter (1995) in the Middle Jurassic formations (Jura Mountains in Switzerland) exhibit comparable characteristics, hosting a variety of encrusters, including serpulids, along with other fossils, including foraminifers and calcisponges. These oncoids feature relatively large nuclei, potentially indicative of the occasional period of relatively higher energy levels during their formation (Burkhalter 1995; Gradzinski *et al*. 2004). In the eastern Sakarya Zone, similar petrographical characteristics of the studied oncoids are observed (Figures 5, 7(a-c)). In addition, fossil assemblage and petrographic characteristics of the oncoids, along with the host rocks, indicate that a significant portion of the sediments was deposited in the shallower part of the slope environment, possibly only a few hundred metres deep (Figure 9(d)).

The host rocks, composed of the ARF strata, are proposed to have been deposited in tilted blocks, slopes, and horsts in pelagic environments (Kandemir and Yılmaz 2009). These facies resemble the widespread

Rosso Ammonitico facies in the Jurassic Tethyan region (Jenkyns 1975; Cecca *et al*. 1992; Barquero *et al*. 2021). Previous studies have often interpreted these facies as being deposited in the slopes of pelagic carbonate platforms (Gradzinski *et al*. 2004; Preat *et al*. 2006; Kandemir and Yılmaz 2009; Reolid and Nieto 2010). This interpretation is consistent with the observations in the current case, where the limestones transition laterally to dark grey marls and shale that were probably deposited in an oxygen-depleted basin. The presence of these different lithologies indicates a dynamic depositional environment characterized by fluctuating hydrological regimes, oxygen levels, element supply, and seawater saturation of specific elements.

Nevertheless, the sedimentary setting of the Eastern Pontides corresponds to seamounts or pelagic isolated platforms during the Early Jurassic (Figure 9(c,d)). The distinct paleoenvironmental conditions can result in a considerable drop in terrigenous influx and reduced sedimentation, which may provide conditions for microbially mediated authigenesis. The presence of biofilm development (Figures 6(a-e) and 7(a-d)), which contributes to the growth of the oncoids, suggests a slow sedimentation rate during the deposition of the host sediment (Gradzinski *et al*. 2004; Reolid *et al*. 2005; Zatoń *et al*. 2012). Similarly, sediment-starved conditions are frequently associated with bacterial stromatolites and sessile foraminifers (Jenkyns 1970; Ballarini *et al*. 1994; Dromart *et al*. 1994; Jiang *et al*. 2019). Similar microbial features, resembling microbialites or oncoids, have been associated with algae, different types of bacteria, and fungi, potentially forming symbiotic relationships (Gradzinski *et al*. 2004; Lindskog 2014). Despite differences in the cortical fabrics observed in the studied oncoids, it is likely that they were all produced by a similar group of organisms, similar to the formation of stromatolites. Although the presence of these oncoids and their distinctive characteristics offers insights into the depositional environment and processes during their formation in the Eastern Pontides Basin, further research is necessary to gain a deeper understanding of the underlying mechanisms and microbial mediation involved under these paleochemical conditions. Investigating their significance within the broader geological context will provide valuable insights into the paleoenvironmental conditions, the availability of element flux (Fe and Mn), seawater saturation, and microbial mediation.

5.2. *Background controls, possible Fe-Mn source, and stratigraphic importance of the Fe-Mn oncoids*

The background controls for the formation of Fe-Mn macro-oncoids are influenced by a combination of various factors, including the specific environmental conditions, the availability of dissolved Fe and Mn in the water column, microbial activity, and physicochemical conditions (e.g. Jenkyns 1970; Vera and Martín-Algarra 2012; Pomoni-Papaioannou 1994; Burkhalter 1995; Preat *et al*. 2000; Salama *et al*. 2013; Reolid and Abad 2019). The availability of iron and manganese in the surrounding environment is a key factor in the formation of Fe-Mn macro-oncoids along with other occurrences such as mineralized coatings and crusts (e.g. Preat *et al*. 2000; Reolid and Nieto 2010; Reolid and Abad 2019; Han *et al*. 2015). However, their source elements are subject to ongoing debate, with several propositions explaining their petrogenesis. These include submarine volcanic activity and/or hydrothermal input (Sturesson *et al*. 2000; Garcia-Frank *et al*. 2012) or continental run-off processes (Palmer and Wilson 1990; Gradzinski *et al*. 2004; Andreeva and Chatalov 2010; Han *et al*. 2015).

The inflow of continental weathering serves as a source of transition metal elements, including Fe and Mn (Gradzinski *et al*. 2004; Özyurt, 2023). This interpretation effectively accounts for the metal element supply for oncoids found in various ironstone deposits located near extensive land masses in England and France (Gatrall *et al*. 1972; Palmer and Wilson 1990). Similarly, the genesis of chamosite from Middle Jurassic ooidal ironstones (southern Tibet) has been linked to intensified continental weathering and erosion, resulting in heightened iron influx into the ocean during transgressive phases marked by reduced sedimentation rates and limited oxygenation at the basin surface (Han *et al*. 2015).

During the Pliensbachian, a significant deepening event in the marine environment is well-documented across various parts of the Tethys Realms (Hallam 1981, 2001; Hesselbo and Jenkyns 1998). A similar transgressive period is marked by the deposition of the ARF in the Eastern Pontides (Kandemir and Yılmaz 2009). The high relative sea levels during this period resulted in a considerable portion of land being submerged, thereby limiting the extent of emergent landmasses. Consequently, the hinterland available for weathering processes could have been comparatively reduced. Therefore, it is questionable to infer that there was adequate land surrounding basins to sustain weathering processes and supply trace elements to the Eastern Pontides Basin. Likewise, certain regions in the Western Carpathians have proposed to be emerged during the Early Jurassic period; their relatively small land area suggests they likely did not supply sufficient elements (Gradzinski *et al*. 2004). Similarly, the limited influx of terrestrial material alongside the presence of ferruginous occurrences has been proposed as a potential alternative source of metals (Kalinina *et al*. 2024). The possible seawater saturation with metals has been attributed to the dissolution of unstable mineral phases from the continent and the potential influence of hydrothermal solutions in the northwestern Caucasus (Kalinina *et al*. 2024)

On the other hand, Lower Jurassic ferromanganese crusts, possessing a chemical composition akin to the discussed oncoids, are attributed to vent activity (Böhm *et al*. 1999). Modern marine Fe-Mn sediments, particularly iron dominating over manganese, are also recorded near submarine hydrothermal vents (Toth 1980Todd *et al*. 2019). Similarly, hydrothermal solutions resulting from rift-related volcanism have been proposed as potential contributors to the formation of Jurassic Fe-Mn occurrences, including mineralized coatings, ooids, crusts, and oncoids in various Tethys Realms. These Jurassic Fe-Mn occurrences, commonly associated with condensed sediments, are widespread across the Western Tethyan Realm, extending from Spain (Reolid and Nieto 2010), northwestern Sicily (Scopellito and Rusco 2021), France (Corbin *et al*. 2000; Preat *et al*. 2000), and northwest Slovenia (Šmuc and Rožič 2010), to the Carpathians (Rojkovič *et al*. 2003; Gradzinski *et al*. 2004). Similar Fe-Mn occurrences are also recorded in the Eastern Tethyan Realm, extending from southern Tibet (Han *et al*. 2015), the Caucasus (Kalinina *et al*. 2024), to Anatolia (Delikan and Orhan 2020). According to these studies, the substantial sources of Fe and Mn can likely be linked to intense syn-sedimentary tectonic activity coinciding with the rifting period or onset of spreading in different parts of the Tethys Ocean.

In the Eastern Pontides, the studied oncoids are hosted in ARF strata that are intercalated with thin-layered volcanic rocks (Kandemir 2004). Thus, the intercalation of ARF strata with thin volcanic rocks can provide important evidence of any volcanic event within the contemporaneous sediments. Additionally, silica enrichment in the cortex layer of the studied oncoid is observed (Supp. File XRD), which can be regarded as evidence of a hydrothermal origin. However, extremely high Ba and Sr contents are reported in such hydrothermal environments (e.g. Usui *et al*. 1997; Reolid and Martínez-Ruiz 2012). The oncoids in ARF strata had relatively lower Ba and Sr contents than those of Fe-Mn crusts in hydrothermal environments (Supplementary Table 1).

The oncoids are situated within the area linked to the Hydrothermal area, as evidenced by the discrimination diagram involving Ni, Co, and Zn (Figure 8a), indicating a hydrothermal source. Both the Ce/CeN versus Nd and Y/HoN discrimination diagrams (Figure 8b,c) show that the oncoids and host rocks are situated in a region associated with hydrothermal Fe and Mn deposits (Alexander *et al*. 2008; Bau *et al*. 2014). Their Eu/Sm ratios, which fall between seawater and hydrothermal fluids, may serve as confirmation of hydrothermal influence (Figure 8d). In the Y/Ho versus Sm/Yb and Eu/Sm diagrams (Figure 8e,f), both the oncoids and host rocks plot within an area which is indicative of hydrothermal fluid influence (Alexander *et al*. 2008; Özyurt *et al*. 2020). Additionally, they exhibit high Eu/Eu* values (corresponding to the positive Eu anomaly), suggesting a slight hydrothermal input to the ambient seawater during their formation. Furthermore, the studied samples exhibit high Ce* and Eu* values, suggesting a potential influence of hydrothermal activity on their formation. However, they show relatively low Sm/Yb, Y/Ho, Eu/Sm, Nd/YbN, and La/Yb values (Figure 8d-f), indicating a limited contribution from hydrothermal sources to the surrounding seawater (Özyurt et al. 2020, 2024).

In accordance with the findings of these studies (Kandemir and Yılmaz 2009), the substantial accumulation of iron (Fe) and manganese (Mn) during this period appears to be linked to heightened syn-sedimentary tectonic activity, coinciding with the onset of spreading in the Eastern sector of the Tethys Ocean. Rift-related volcanism may occasionally provide hydrothermal solutions, and these processes likely introduced Fe, Mn, trace elements, and REE into seawater. The saturation of metals in seawater can promote the formation of these oncoids. The processes might have been repeated several times, interrupting the mineralization in the context. This is evidenced by the oncoid's cortex exhibiting a diverse chemical composition (Figures 6a-h and 7e-h). Thus, the studied Fe-Mn oncoids might have been formed in a tectonically active basin where extensional tectonic movements continuously affected paleoenvironmental conditions (Kandemir and Yılmaz 2009).

On the other perspective, similar macro-oncoids resembling microfilamentous or spongy networks, possibly representing fossilized fungal mats, have been documented in a different part of the Jurassic Tethys (e.g. Tyszka and Kaminski 1995; Gradzinski *et al*. 2004; Reolid and Nieto 2010). These oncoid-bearing layers are located below the radiolarites in that particular Jurassic Tethyan region. In the study area, the studied section displays typical characteristics of a transgressive sequence, including a fining-upward trend, an increase in the amount of clay matrix towards the top of the sequence, a gradual decrease in shallow-water forms, and an abundance of radiolarians in the nodular marly facies located at the uppermost part of the section (Kandemir and Yılmaz 2009). Additionally, the oncoid-bearing layers in the studied section are located at the upper part, just below the marly facies (Kandemir and Yılmaz

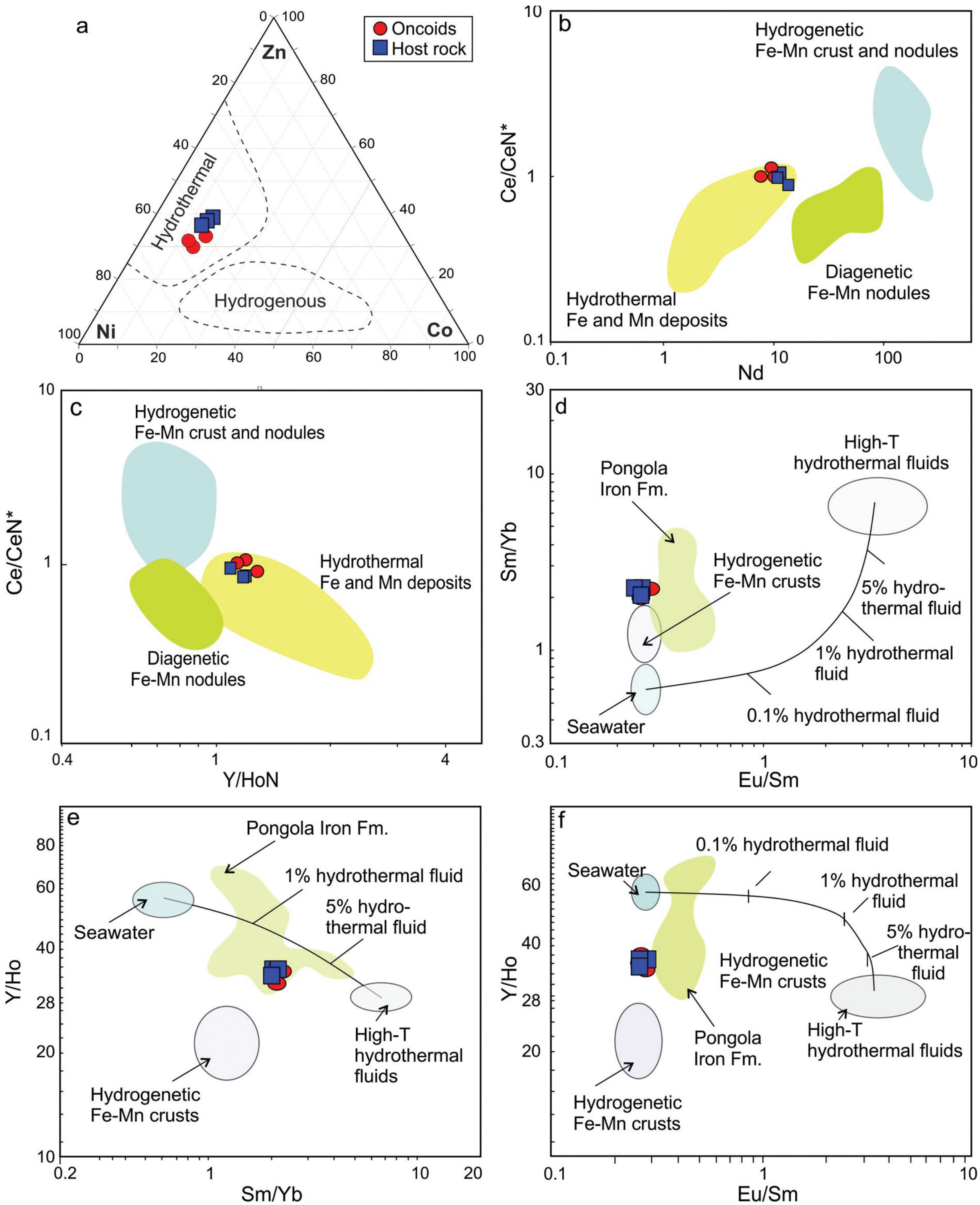

Figure 8. Plots of the Eu/Sm vs. Sm/Yb (a); Sm/Yb vs. Y/Ho ((b); Eu/Sm vs. Y/Ho (c); Zn–Co–Ni(d) Nd vs Ce/Ce* (e) (Y/ho)n vs. Ce/Ce* (f). The diagrams displaying end member-component mixing (a, b, c) are adapted from Alexander et al. (2008), Özyurt et al. (2020), and references therein. The ternary discrimination diagram (d) is based on Choi and Hariya (1992), Khan et al. (2020), and references therein. The bivariate discrimination diagrams (e, f) follow the approach outlined by Bau et al. (2014).

2009). The similar stratigraphic position of the oncoid-bearing layers and the presence of similar oncoids with comparable petrochemical characteristics in both the eastern and western parts of the Tethyan basin highlights their palaeogeographic and stratigraphic significance.

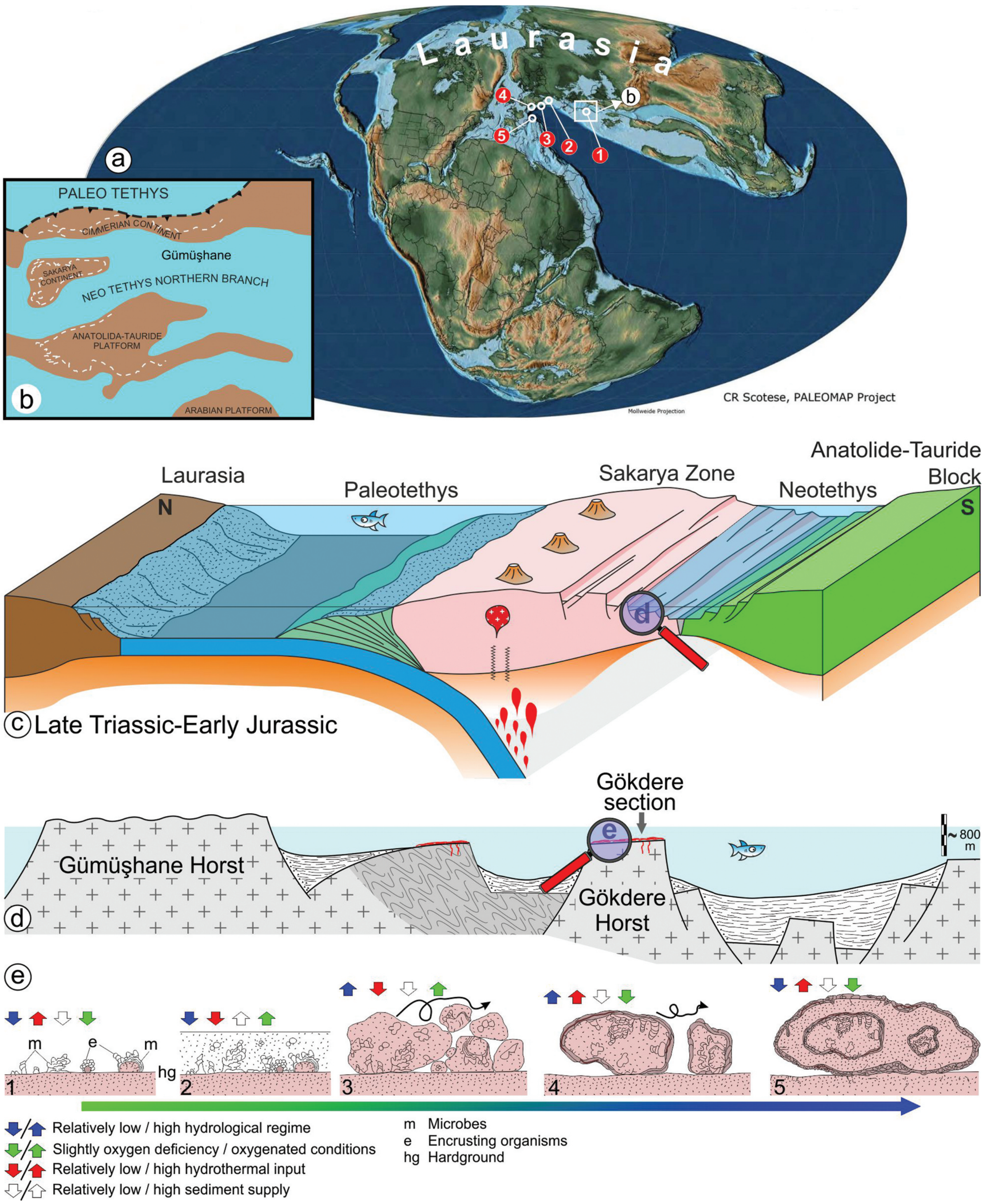

Figure 9. a: Global palaeographic reconstruction of the Earth in the Early Jurassic period (1: This study, 2: Gradzinski et al. 2004, 3; Cronan et al. 1991, 4; Böhm et al. 1999, 5; Preto et al. 2017; the reconstruct map from Scotese, 2021); b: Detailed palaeographic map of the eastern Sakarya Zone (from Şengör and Yilmaz 1981); c-d: Palaeogeographic position of the studied basins at Late Triassic-Early Jurassic time span from (Kandemir et al. 2022); e: Sequence of evolution of the nodules (1- growth of microbes (m) and encrusting processes on a hardground (hg); 2- deposition of pelagic sediment and burial of microbial and encrusting processes; 3- formation of clasts by burrowing and/or currents; 4- encrustation of isolated clasts and and rolling under currents; 5- development of microbial lamination and encrusting processes; 6- renewed growth of microbes (m) and encrusting organisms on the oncoid, modified from Flügel (2004).

5.3. Implications for interplay of distinct paleoenvi ronmental conditions and tectono-sedimentary evolution of the eastern Sakarya Zone

The geotectonic evolution of the eastern Sakarya Zone in NE Turkey, situated within the Alp orogenesis belt, has been debated. Researchers have proposed two contrasting views. One perspective suggests that the eastern Sakarya Zone was part of Gondwana's northern margin, facing the Paleotethys during the Late Paleozoic (Şengör *et al*. 1980; Görür *et al*. 1983; Yılmaz *et al*. 1997; Dokuz *et al*. 2017; Karsli *et al*. 2017). This view indicates the southward subduction of the Paleotethys from the Permian to the middle Jurassic, leading to the opening of Neotethyan oceanic basins south of the Cimmeria continent and behind Gondwana's northern margin (Şengör 1979; Şengör *et al*. 2023). The Middle Jurassic witnessed the collision of the southern margin of Laurasia with the eastern Sakarya Zone, with Neo-Tethys Ocean remaining in the Tethyan realm (Şengör 1984) and collision-related granites in Artvin area (Dokuz *et al*. 2010). On the other hand, an alternative model proposes that the Pontides were located at the southern margin of Laurasia, facing the Tethyan Ocean in the south (Robertson and Dixon 1984; Robinson *et al*. 1995; Okay and Sahinturk 1997; Okay 2000). This view suggests an Andean-type margin for the southern margin of Laurasia (Pontides), with Paleotethys subduction occurring from the late Palaeozoic to Palaeocene, eventually leading to the collision of the eastern Sakarya Zone with the Anatolide-Tauride Block during the Paleocene (Okay 2000).

Both conflicting models proposed implications for the rift-related- deposition of the Early-Middle Jurassic volcano-sedimentary successions in the eastern Sakarya Zone. This topic has been extensively discussed by numerous researchers, focusing on the Early Jurassic rifting throughout the region for decades (Şengör and Yilmaz 1981; Görür *et al*. 1983; Yılmaz *et al*. 1997; Koçyiğit and Altıner 2002; Yilmaz and Kandemir 2006; Dokuz *et al*. 2017; Dokuz and Sünnetçi 2019). Recently, Karsli *et al*. (2017) and Dokuz and Sünnetçi (2019) have reported early Jurassic acidic magmatic rocks in the eastern Sakarya Zone, suggesting a back-arc setting during the southward subduction of the Paleotethys oceanic lithosphere, which likely contributed to the generation of early Jurassic magmatic rocks. More recently, Kandemir *et al*. (2022) proposed that the Lower Jurassic sandstone succession likely marks the transition from a rifted to a passive margin. The rifting process has been proposed to be initiated in the southern margin of the arc, leading to the formation of an intra-arc rift parallel to the continental margin, together with the development of the Neotethyan basin to the south (Şengör and Yilmaz 1981; Şen 2007; Dokuz and Sünnetçi 2019; Kandemir *et al*. 2022). The studied oncoids are hosted in the Ammonitico Rosso type carbonates, which overlie the sandstone succession in the studied measured section and the other localities in the eastern Sakarya Zone (Figure 2). Kandemir and Yılmaz (2009) indicate that these carbonates were developed during the rifting of the continental margins, exhibiting the phases of the Tethys opening (Figure 9a-c). This study also notes that the deposition was controlled by the syn-depositional tectonic regime, and the carbonates accumulated on tilted block tops, slopes, and horsts in an open marine environment (Figure 9d).

Similarly, Kandemir (2004) also describes that Neptunian dykes formed at the different levels of the Ammonitico Rosso type carbonates were filled with overlying sediments and also provide evidence that the extensional tectonic movements continuously influence the basin during the sedimentation of the carbonates. This extension must be developed in a back-arc environment during the early Jurassic (Figure 9a-d). As the basin gradually deepened and the tectonic activity possibly decreased, it created a favourable environment for the deposition of the last part of Ammonitico Rosso facies and overlying shales, which are abundantly represented in the upper part of the Lower Jurassic successions. This suggests a dynamic sedimentary evolution with distinct environmental conditions that triggered the formation of Fe-Mn oncoids in the region.

On the other hand, Fe and Mn influx are generally associated with hydrothermal plumes located on mid-oceanic ridge flanks (German *et al*. 1990; Edmonds and Edmond 1995; Corbin *et al*. 2000), exerting their influence over several hundred kilometres on each side of the ridge. In addition, former studies (Gerard and Person 1994; Preat *et al*. 2000; Corbin *et al*. 2000; Gradzinski *et al*. 2004; Reolid and Nieto 2010; Scopellito and Rusco 2021; Han *et al*. 2023; Kalinina *et al*. 2024) have demonstrated that possible hydrothermal circulations related to syn-rift fault systems could contribute noticeably to the element supplies in seawater. In the eastern Sakarya Zone, the occasional syn-depositional extensional movement might have provided hydrothermal fluid input to marine environments, leading to enrichment in saturation of metals in seawater. Under these circumstances, the oncoids were formed through the meditation of microbial organisms (bacteria and fungi?) and encrusting fossils, along with the deposition of host rock with foraminifers containing benthic and planktonic association Figures 3(e,f), 4(d-f), and 6(b-f).

In addition, Delikan and Orhan (2020) have conducted a study on pelagic carbonates in the vicinity of Ankara in central Anatolia. They have proposed that a pelagic carbonate platform was deposited in a basin affected by synsedimentary faulting, leading to the formation of condensed, nodular, pelagic oolitic-ammonitic limestones in open-marine environments. The Early-Middle Jurassic sequences in the region pass upward into thick-bedded, shallow marine oolitic limestone, specifically of Callovian age, known as the Berdiga Formation (Pelin 1977). In the eastern Sakarya Zone, the Senköy Formation is known to be conformably overlaid by platform carbonates of the Berdiga Formation (Pelin 1977). Throughout the early Cretaceous, carbonate sedimentation dominates in the basin (Pelin 1977; Özyurt *et al*. 2019a, 2019b, 2019c, 2020, 2022, 2023, our unpublished data), which would be challenging to explain without any clastic input in a foreland basin over a subduction zone. Conversely, such depositions are more feasible on the passive margin of a marginal basin (Figure 9). In another study on the eastern Sakarya Zone, Dokuz *et al*. (2017) suggested that the presence of basaltic sills within the formation indicates back-arc extension in the south, which eventually led to the break-up of the arc in the North.

More recently, Azizi *et al*. (2023) have presented a comprehensive correlation between Early to Middle Jurassic magmatism and sedimentation in Iran and Turkey and have proposed the region experienced an extensional tectonic regime during this time, forming a continental rift that later evolved into a passive margin on the southwestern margin of Eurasia. The sedimentological pieces of evidence for the opening history of the northern branch of the Neo-Tethys and its early Jurassic-Aptian evolution have been previously documented by Görür *et al*. (1983). Then, a line parallel to the magmatic arc in the north has been described as the North Anatolian Paleorift (NAPR) line by Koçyiğit and Altıner (2002). It is also interpreted as a south-facing passive continental margin of the northern Neotethys (e.g. Azizi *et al*. 2018; Azizi and Stern 2019; Nouri *et al*. 2023). Combined with our sedimentological data and previous research, these observations suggest a dynamic evolution of the basin in the eastern Sakarya Zone, influencing changes in paleoenvironmental conditions and shaping sedimentary processes. The complex function of these sedimentary factors has led to the generation of Fe-Mn oncoids over time (Figure 9e).

6. Conclusions

Based on detailed sedimentological and geochemical analyses of the oncoids in the Early Jurassic (Pliensbachian) ARF strata of the eastern Sakarya Zone (NE Turkey), specific paleoenvironmental conditions can be inferred, characterized by submarine topographic highs or isolated pelagic platforms. These conditions entail prolonged seafloor exposure, slow sedimentation rates, fluctuating oxygen levels, and hydrologic regime (a mildly agitated to stable), along with the presence of iron (Fe) and other metals and REE. These conditions probably create an environment conducive to the development of hardgrounds and the formation of oncoids, with several key points that can be concluded:

(1) The oncoids, varying in size from 10 to over 45 mm, display a spectrum of colours, including brown, reddish, and metallic hues, and typically exhibit a discoidal shape, occasionally spherical. Their nuclei, composed of bioclastic wackestones containing remnants of ammonoid shells, may include multiple nuclei in certain discoidal forms. The cortex of the oncoids is characterized by wrinkled bands displaying micritic laminae, often with filamentous bodies, and sporadically encrusted with microfossils. In the cortex, iron predominates over manganese, with significant compositional variations, particularly enriched in Si, Fe, and Ca.

(2) These oncoids align predominantly with the plot associated with hydrothermal Fe and Mn sediments, as indicated by discrimination diagrams involving Ni, Co, Zn, and plots of Ce/Ce* vs. Y/HoN and Nd contents, suggesting a hydrothermal origin. Additionally, their REE chemistry exhibits distinct Y/Ho, Sm/Yb, Ce/Ce, and Nd values, suggesting the influence of seawater mixing with hydrothermal fluids. However, they show relatively low Sm/Yb, Y/Ho, Eu/Sm, Nd/YbN, and La/Yb values, suggesting a limited contribution from hydrothermal sources to the surrounding seawater. Syn-depositional extensional movements likely facilitated the input of hydrothermal fluids into marine environments, contributing to the specific element saturation of seawater. In such environments, the genesis of oncoids is shaped by a complex interplay of sedimentary factors, including the availability of metal sources, prevailing dynamic paleoenvironmental conditions, and the presence of microbial organisms.

(3) The occurrence of oncoid-bearing layers at consistent stratigraphic positions, coupled with the presence of similar oncoids exhibiting comparable petrographic characteristics across both the eastern and western regions of the Tethyan basin, underscores their profound implications for palaeogeography and stratigraphy.

Acknowledgments

The authors acknowledge the Recep Tayyip Erdogan University and Karadeniz Technical University for facilitating sedimentology research. Serdar Görkem Atasoy from Middle East Technical University is also acknowledged for his contribution to the palaeontological aspect of this paper. We would like to acknowledge Dr. Tuğba Bayazit (Recep Tayyip Erdoğan University) for her assistance with the SEM analyses.

Disclosure statement

No potential conflict of interest was reported by the author(s).

Funding

The author(s) reported there is no funding associated with the work featured in this article.

References

Akkemik, Ü., Kandemir, R., Philippe, M., Güngör, Y., and Köroğlu, F., 2022, Palaeobiogeographical implications of the first fossil wood flora from the Jurassic of Turkey: Acta Palaeontologica Polonica, no. 3, v. 67, p. 745–766. doi: 10.4202/app.00962.2021

Alexander, B.W., Bau, M., Andersson, P., and Dulski, P., 2008, Continentally-derived solutes in shallow Archean seawater: Rare earth element and Nd isotope evidence in iron formation from the 2.9 Ga Pongola Supergroup, South Africa: Geochimica et Cosmochimica Acta, no. 2, v. 72, p. 378–394. doi: 10.1016/j.gca.2007.10.028

Alkaya, F., and Meister, C., 1995, Liassic ammonites from the central and eastern Pontides (Ankara and Kelkit areas, Turkey): Revue de Paléobiologie, no. 1, v. 14, p. 125–193

Andreeva, P., and Chatalov, A., 2010, Origin of the Eifellian Ironstons from R-119 Kardam, Northeastern Bulgaria: Geologie Sedimentologie, no. 1, v. 64, p. 91–101

Azizi, H., Lucci, F., Stern, R.J., Hasannejad, S., and Asahara, Y., 2018, The Late Jurassic Panjeh submarine volcano in the northern Sanandaj-Sirjan Zone, northwest Iran: Mantle plume or active margin?: Lithos, v. 308, p. 364–380. doi: 10.1016/j.lithos.2018.03.019

Azizi, H., and Stern, R.J., 2019, Jurassic igneous rocks of the central Sanandaj–Sirjan zone (Iran) mark a propagating continental rift, not a magmatic arc: Terra Nova, no. 5, v. 31, p. 415–423. doi: 10.1111/ter.12404

Azizi, H., Stern, R.J., Kandemir, R., and Karsli, O., 2023, A Jurassic volcanic passive margin in Iran and Turkey: Terra Nova, no. 3, v. 35, p. 141–152. doi: 10.1111/ter.12638

Badenas, B., and Aurell, M., 2010, Facies models of a shallow-water carbonate ramp based on distribution of non-skeletal grains (Kimmeridgian, Spain): Facies, no. 1, v. 56, p. 89–110. doi: 10.1007/s10347-009-0199-z

Ballarini, L., Massari, F., Nardi, S., and Scudeler, B.L., 1994, Amino acids in the pelagic stromatolites of the rosso ammonitico veronese formation (Middle-Upper Jurassic, Southern Alps, Italy), *in* Bertrand-Sarfati, J., and Monty, C., eds. Phanerozoic stroma tolites II: Amsterdam, Kluwer Academic Publishers, pp. 279–282.

Barquero, A.S., Sáez, F.O., Jiménez, A.G., and Barrionuevo, F.J.G., 2021, The Ammonitico Rosso Facies in Sierras Subbéticas UGGp: Córdoba, Spain, Geological Importance and Threats–The Case of La Cañada del Hornillo.

Bau, M., and Dulski, P., 1996, Distribution of yttrium and rare-earth elements in the Penge and Kuruman iron-formations, Transvaal supergroup, South Africa: Precambrian Research, v. 79, no. 1–2, p. 37–55.

Bau, M.S.K.K., Schmidt, K., Koschinsky, A., Hein, J., Kuhn, T., and Usui, A., 2014, Discriminating between different genetic types of marine ferro-manganese crusts and nodules based on rare earth elements and yttrium: Chemical Geology, v. 381, p. 1–9. doi: 10.1016/j.chemgeo.2014.05.004

Birkenmajer, K., 2001, Mesozoic and Cenozoic stratigraphic units in pARF of the South Shetland Islands and Northern Antarctic Peninsula (as used by the Polish Antarctic Programmes): Studia Geologica Polonica, v. 118, p. 5–188.

Böhm, F., and Brachert, T.C., 1993, Deep-water stromatolites and Frutexites Maslov from the Early and Middle Jurassic of S-Germany and Austria: Facies, no. 1 v. 28, p. 145–168. doi: 10.1007/BF02539734

Böhm, F., Ebli, O., Krystyn, L., Lobitzer, H., Raku's, M., and Siblik, M., 1999, Fauna, stratigraphy and depositional environment of the Hettangian-Sinemurian (Early Jurassic) of Adnet (Salzburg, Austria): Abhandlungen der Geologischen Bundesanstalt, v. 56, p. 143–271.

Boynton, W.V., 1984, Cosmochemistry of the rare earth elements: Meteorite studies, *in* Developments in geochemistry, Elsevier, v. 2, 63–114p.

Burkhalter, R.M., 1995, Ooidal ironstones and ferruginous microbialites: Origin and relation to sequence stratigraphy (Aalenian and Bajocian, Swiss Jura mountains): Sedimentology, no. 1, v. 42, p. 57–74. doi: 10.1111/j.1365-3091.1995.tb01271.x

Çapkınoğlu, Ş., 2003, First Records of Conodonts from"The Permo-Carboniferous of Demirözü"(Bayburt), Eastern Pontides, NE Turkey: Turkish Journal of Earth Sciences, no. 2, v. 12, p. 199–207

Cecca, F., Fourcade, E., and Azéma, J., 1992, The disappearance of the "Ammonitico Rosso": Palaeogeography, Palaeoclimatology, Palaeoecology, no. 1–2, v. 99, p. 55–70. doi: 10.1016/0031-0182(92)90007-R

Choi, J.H., and Hariya, Y., 1992, Geochemistry and depositional environment of Mn oxide deposits in the Tokoro Belt, northeastern hokkaido, Japan: Economic Geology, v. 87, no. 5, no. 1265–1274.

Cirilli, Iannace, Jadoul, and Zamparelli, 1999, Microbial–serpulid build-ups in the Norian–Rhaetian of the Western Mediterranean area: Ecological response of shelf margin communities to stressed environments: Terra Nova, no. 5, v. 11, p. 195–202. doi: 10.1046/j.1365-3121.1999.00245.x

Corbin, J.C., Person, A., Iatzoura, A., Ferre, B., and Renard, M., 2000, Manganese in pelagic carbonates: Indication of major tectonic events during the geodynamic evolution of a passive continental margin (the Jurassic European margin of the Tethys–Ligurian Sea): Palaeogeography, Palaeoclimatology, Palaeoecology, no. 1–2, v. 156, p. 123–138. doi: 10.1016/S0031-0182(99)00135-2

Cronan, A.S., Galacz, A., Mindszenty, A., Moory, S.A., and Polgari, M., 1991, Tethyan ferromanganese oxide deposits from Jurassic rocks in Hungary: Journal of the Geological

Society, no. 4, p. v. 148, 655–668. doi: 10.1144/gsjgs.148.4.0655

Delikan, A., and Orhan, H., 2020, Sedimentology of Jurassic pelagic carbonate platforms in the Ankara region (Central Anatolia-Turkey): Facies, no. 3, v. 66, p. 19. doi: 10.1007/s10347-020-00603-y

Dokuz, A., Aydınçakır, E., Kandemir, R., Karslı, O., Siebel, W., Derman, A.S., and Turan, M., 2017, Late Jurassic magmatism and stratigraphy in the eastern Sakarya zone, Turkey: Evidence for the slab breakoff of Paleotethyan oceanic lithosphere: The Journal of Geology, no. 1, v. 125, p. 1–31. doi: 10.1086/689552

Dokuz, A., Karsli, O., Chen, B., and Uysal, İ., 2010, Sources and petrogenesis of Jurassic granitoids in the Yusufeli area, Northeastern Turkey: Implications for pre-and post-collisional lithospheric thinning of the eastern Pontides: Tectonophysics,no. 1–4, v. 480, p. 259–279. doi: 10.1016/j.tecto.2009.10.009

Dokuz, A., and Sünnetçi, K., 2019, Jurassic acidic magmatism in a back-arc setting, eastern Sakarya Zone, Turkey: Geochemical constraints and an evolutionary model: Lithos, v. 332, p. 312–327. doi: 10.1016/j.lithos.2019.02.022

Dromart, G., Gaillard, C., and Jansa, L.F., 1994, Deep-marine microbial struc tures in the Upper Jurassic of Western Tethys, *in* Bertrand Sarfati, J., and Monty, C., eds. Phanerozoic stromatolites II: Amsterdam, Kluwer Academic Publishers, pp. 295–318

Edmonds, H.N., and Edmond, J.M., 1995, A three-component mixing model for ridge-crest hydrothermal fluids: Earth and Planetary Science Letters, no. 1–2, v. 134, p. 53–67. doi: 10.1016/0012-821X(95)00115-S

Flügel, E., 2004, Microfacies of carbonate rocks. Analysis, interpretation and application: Berlin, Heidelberg, New York, Springer-Verlag, p. xx +976. doi: 10.1017/S0016756806221940

Flügel, E., 2012, Microfacies analysis of limestones, Springer Science & Business Media

Fornós, J.J., Forteza, V., and Martínez-Taberner, A., 1997, Modern polychaete reefs in Western Mediterranean lagoons: Ficopomatus enigmaticus (Fauvel) in the Albufera of Menorca, Balearic Islands, Palaeogeography, Palaeoclimatology, Palaeoecology, no. 1–4, v. 128, p. 175–186. doi: 10.1016/S0031-0182(96)00045-4

Friebe, J.G., 1994, Serpulid-bryozoan-foraminiferal biostromes controlled by temperate climate and reduced salinity: Middle Miocene of the Styrian Basin, Austria: Facies, no. 1 v. 30, p. 51–62. doi: 10.1007/BF02536889

Garcia-Frank, A., Ureta, S., and Mas, R., 2012, Iron-coated particles from condensed Aalenian–bajocian deposits: Evolutionary model (iberian basin, Spain): Journal of Sedimentary Research, v. 82, no. 12, p. 953–968.

Gatrall, M., Jenkyns, H.C., and Parsons, C.F., 1972, Limonitic concretions from the European Jurassic, with particular reference to the “snuff-boxes” of southern England: Sedimentol, no. 1–2 v. 18, p. 79–103. doi: 10.1111/j.1365-3091.1972.tb00004.x

Gerard, M., and Person, A., 1994, Low hydrothermal impact in volcaniclastic sediments of the North Aoba Basin: Sites 832 and 833. In Proceedings of the Ocean Drilling Program. Scientific results, TX, United States, Ocean Drilling Program, College Station, Vol. 134, pp. 131–176.

German, C.R., Klinkhammer, G.P., Edmond, J.M., Mura, A., and Elderfield, H., 1990, Hydrothermal scavenging of rare-earth elements in the ocean: Nature, no. 6275, v. 345, p. 516–518. doi: 10.1038/345516a0

Ghiorse, W.C., and Ehrlich, H.L., 1992, Microbial biomineralization of iron and manganese: Catena, Supplement, v. 21, p. 75–99

Golubic, S., Campbell, S.E., Drobne, K., Cameron, B., Balsam, W. L., Cimerman, F., and Dubois, L., 1984, Microbial endoliths: A benthic overprint in the sedimentary record, and a paleobathymetric cross-reference with foraminifera: Journal of Paleontology, v. 58, no. 2 , p. 351–361.

Görür, N.A., Şengör, A., Akkök, R., and Yılmaz, Y., 1983, Sedimentological evidence for the opening of the northern branch of Neo - Tethys in the Pontides: Bulletin of the Geological Society of Turkey, v. 26, p. 11–20

Gradzinski, M., Tyszka, J., Uchman, A., and Jach, R., 2004, Large microbial-foraminiferal oncoids from condensed Lower–Middle Jurassic deposits: A case study from the Tatra Mountains, Poland: Palaeogeography, Palaeoclimatology, Palaeoecology, no. 1–2, v. 213, p. 133–151. doi: 10.1016/j.palaeo.2004.07.010

Hägele, D., Leinfelder, R., Grau, J., Burmeister, E.G., and Struck, U., 2006, Oncoids from the river Alz (southern Germany): Tiny ecosystems in a phosphorus-limited environment: Palaeogeography, Palaeoclimatology, Palaeoecology, no. 2–4, v. 237, p. 378–395. doi: 10.1016/j.palaeo.2005.12.016

Hallam, A., 1981, A revised sea-level curve for the early jurassic: Journal of the Geological Society, v. 138, no. 6, p. 735–743.

Hallam, A., 2001, A review of the broad pattern of Jurassic sea-level changes and their possible causes in the light of current knowledge: Palaeogeography Palaeoclimatology Palaeoecology, no. 1–2, v. 167, p. 23–37. doi: 10.1016/S0031-0182(00)00229-7

Han, Z., Zhang, X., Chi, N., Han, M., Woo, J., Lee, H.S., and Chen, J., 2015, Cambrian oncoids and other microbial-related grains on the North China Platform, Carbonates and Evaporites, no. 4, v. 30, p. 373–386. doi: 10.1007/s13146-014-0209-2

Hesselbo, S.P., and Jenkyns, H.C., 1998, British Lower Jurassic sequence stratigraphy, *in* de Graciansky, P.C., Hardenbol, J., Jacquin, T., Farley, M., and Vail, P.R., eds. Mesozoic-Cenozoic Sequence Stratigraphy of European Basins, SEPM Special Publication No. 60: Society for Sedimentary Geology, pp. 561–581.

Jach, R., and Starzec, K., 2003, Glaucony from the condensed Lower-Middle Jurassic deposits of the Križna Unit, Western Tatra Mountains, Poland: Annales Societatis Geologorum Poloniae, v. 73, no. 3, p. 183–192.

Jenkyns, H.C., 1970, Fossil manganese nodules from the west Sicilian Jurassic: Eclogae Geologicae Helvetiae, v. 63, no. 3, p. 741–774

Jenkyns, H.C., 1975, Origin of red nodular limestones (Ammonitico Rosso, Knollenkalke) in the Mediterranean Jurassic: A diagenetic model, Pelagic Sediments: On Land and Under the Sea: Wiley Online Library, p. 249–271

Jiang, X.-D., Sun, X.-M., and Guan, Y., 2019, Biogenic mineralization in the ferromanganese nodules and crusts from the South China Sea: Journal of Asian Earth Sciences, v. 171, p. 46–59. doi: 10.1016/j.jseaes.2017.07.050

Jones, R.W., 1984, Comparison of carbonate and shale source rocks: AAPG Bulletin, v. 68, no. 4, p. 163–180. doi: 10.1306/AD460EA4-16F7-11D7-8645000102C1865D

Jones, B., and Renaut, R.W., 1997a, Formation of silica oncoids around geysers and hot springs at El Tatio, northern Chile: Sedimentology, v. 44, no. 2, p. 287–304. doi: 10.1111/j.1365-3091.1997.tb01525.x

Jones, B., and Renaut, R.W., 1997b, Microbial structures in the saline, alkaline, ephemeral lakes of the Cariboo Plateau, British Columbia, Canada: Sedimentary Geology, v. 113, no. 1–2, p. 13–36

Kalinina, N., Maximov, P., Molukpayeva, D., Sherstyukov, M., Kerimov, A.G., and Rudmin, M., 2024, Depositional palaeoenvironment of the Middle Jurassic (Aalenian) ooidal ironstones in Labino-Malkin zone (north-western Caucasus): Marine and Petroleum Geology, v. 162, p. 106744. doi: 10.1016/j.marpetgeo.2024.106744

Kandemir, R. (2004). Gümüşhane ve yakın yörelerindeki erken-orta jura yaşlı şenköy formasyonu'nun çökel özellikleri ve birikim koşulları [Phd Thesis]. Turkish Karadeniz Technical University, Trabzon.

Kandemir, R., and Lerosey-Aubril, R., 2011, First report of a trilobite in the Carboniferous of Eastern Pontides, NE Turkey: Turkish Journal of Earth Sciences, v. 20, no. 2, p. 179–183. doi: 10.3906/yer-0911-3

Kandemir, R., Özyurt, M., and Karsli, O., 2022, Sedimentological and geochemical characteristics of Lower Jurassic Sandstones from Gümüşhane, NE Turkey: Implications for source to sink processes, paleoenvironmental conditions, provenance and tectonic settings: International Geology Review, v. 64, no. 12, p. 1719–1742. doi: 10.1080/00206814.2021.1958383

Kandemir, R., and Yılmaz, C., 2009, Lithostratigraphy, facies, and deposition environment of the lower Jurassic Ammonitico Rosso type sediments (ARTS) in the Gümüşhane area, NE Turkey: Implications for the opening of the northern branch of the Neo-Tethys Ocean: Journal of Asian Earth Sciences, v. 34, no. 4, p. 586–598. doi: 10.1016/j.jseaes.2008.08.006

Karsli, O., Dokuz, A., and Kandemir, R., 2017, Zircon Lu-Hf isotope systematics and U–Pb geochronology, whole-rock Sr-Nd isotopes and geochemistry of the early Jurassic Gokcedere pluton, Sakarya Zone-NE Turkey: A magmatic response to roll-back of the Paleo-Tethyan oceanic lithosphere: Contributions to Mineralogy and Petrology, v. 172, p. 1–27, no. 5. doi: 10.1007/s00410-017-1346-0

Karsli, O., Dokuz, A., Uysal, İ., Aydin, F., Chen, B., Kandemir, R., and Wijbrans, J., 2010, Relative contributions of crust and mantle to generation of Campanian high-K calc-alkaline I-type granitoids in a subduction setting, with special reference to the Harşit Pluton, Eastern Turkey: Contributions to Mineralogy and Petrology, v. 160, p. 467–487, no. 4. doi: 10.1007/s00410-010-0489-z

Khan, M.A., Kakar, M.I., Ulrich, T., Ali, L., Kerr, A.C., Mahmood, K., and Siddiqui, R.H., 2020, Genesis of manganese deposits in the Ali Khanzai block of the Zhob ophiolite, Pakistan: Inferences from geochemistry and mineralogy: Journal of Earth Science, v. 31, p. 884–895.

Kırmacı, M.Z., Koch, R., and Bucur, J.I., 1996, An Early Cretaceous section in the Kircaova Area (Berdiga Limestone, NE-Turkey) and its correlation with platform carbonates in W-Slovenia: Facies, v. 34, p. 1–21. doi: 10.1007/BF02546154

Koçyiğit, A., and Altıner, D., 2002, Tectonostratigraphic evolution of the North Anatolian Palaeorift (NAPR): Hettangian-Aptian passive continental margin of the northern Neo-Tethys, Turkey: Turkish Journal of Earth Sciences, v. 11, no. 3, p. 169–191

Konhauser, K.O., 1998, Diversity of bacterial iron mineralization: Earth-Science Reviews, v. 43, no. 3–4, p. 91–121. doi: 10.1016/S0012-8252(97)00036-6

Lazăr, I., Grădinaru, M., and Petrescu, L., 2013, Ferruginous microstromatolites related to Middle Jurassic condensed sequences and hardgrounds (Bucegi Mountains, Southern Carpathians, Romania): Facies, v. 59, p. 359–390, no. 2. doi: 10.1007/s10347-012-0313-5

Lencina, A.I., Soria, M.N., Colla, M.F., Cury, L.F., FaríFaríAs, M.E., and Gomez, F.J., 2023, In situ growth of modern 960 oncoids from Salado river, Salar de la Laguna Verde Complex, Argentina: Sedimentary Geology, v. 451, p. 106396. doi: 10.1016/j.sedgeo.2023.106396

Lindskog, A., 2014, Palaeoenvironmental significance of cool-water microbialites in the Darriwilian (Middle Ordovician) of Sweden: Lethaia, v. 47, no. 2, p. 187–204. doi: 10.1111/let.12050

Logan, B.W., Rezak, R., and Ginsburg, R.N., 1964, Classification and Environmental Significance of Algal Stromatolites: The Journal of Geology, v. 72, p. 68–83, no. 1. doi: 10.1086/626965

Massari, F., and Dieni, I., 1983, Pelagic oncoids and ooids in the Middle–Upper Jurassic of Eastern Sardinia, *in* Peryt, T., ed. Coated Grains: Berlin, Springer-Verlag, pp. 367–376

Misik, M., and Sucha, V., 1997, Chlorite and Chlorite-Hematite Oncoids from the Jurassic limestones of the western Carpathians, Slovakia: Geologica Carpathica, v. 48, no. 2, p. 85–98

Monty, C., 1984, Cavity and fissure dwelling stromatolites (endostromatolites) from Belgian Devonian mud mounds: Annales Société Géologique Belgique, v. 105, p. 343–344

Nouri, F., Azizi, H., Stern, R.J., and Asahara, Y., 2023, The Sanandaj-Sirjan Zone (W. Iran) was a Jurassic passive continental margin: Evidence from igneous rocks of the Songhor area: Lithos, v. 440-441, p. 107023. doi: 10.1016/j.lithos.2023.107023

Okay, A.I., 1984, Distribution and characteristics of the north-west Turkish blueschists: Geological Society, London, Special Publications, v. 17, no. 1, p. 455–466

Okay, A.I., 2000, Was the Late Triassic orogeny in Turkey caused by the collision of an oceanic plateau?: Geological Society, London, Special Publications, v. 173, no. 1, p. 25–41. doi: 10.1144/GSL.SP.2000.173.01.02

Okay, A.I., and Leven, E.J., 1996, Stratigraphy and paleontology of the upper Paleozoic sequences in the Pulur (Bayburt) region, Eastern Pontides: Turkish Journal of Earth Sciences, v. 5, no. 2, p. 145–155. doi: 10.55730/1300-0985.1744

Okay, A.I., and Sahinturk, O., 1997 , AAPG Memoir 68: Regional and Petroleum Geology of the Black Sea and Surrounding Region: Chapter 15, The AAPG/Datapages Combined Publications Database, AAPG Special Volumes, Geology of the Eastern Pontides.

Okay, A.I., and Tüysüz, O., 1999, Tethyan sutures of northern Turkey: Geological Society, London, Special Publications, v. 156, no. 1, p. 475–515. doi: 10.1144/GSL.SP.1999.156.01.22

Olivier, N., Colombié, C., Pittet, B., and Lathuilière, B., 2011, Microbial carbonates and corals on the marginal French

Jura platform (Late Oxfordian, Molinges section): Facies: v. 57, p. 469–492, no. 3. doi: 10.1007/s10347-010-0246-9

Özyurt M., 2023, Geochemistry of the Aptian bituminous limestones in Gümüşhane area, Eastern Black Sea region: new insight into paleogeography and paleoclimate conditions: Acta Geochim, v. 42, no. 6, p. 971–987. doi: 10.1007/s11631-023-00623-9

Özyurt, M., Al-Aasm, I.S., and Ziya Kirmaci, M., (2019a), Diagenetic Evolution of Upper Jurassic-Lower Cretaceous Berdiga Formation, NE Turkey: Petrographic and Geochemical Evidence, *in* Paleobiodiversity and Tectono-Sedimentary Records in the Mediterranean Tethys and Related Eastern Areas: Proceedings of the 1st Springer Conference of the Arabian Journal of Geosciences (CAJG-1), Tunusıa, 2018: Springer International Publishing, pp. 175–177.

Özyurt, M., Kandemir, R., and Yıldızoğlu, S., 2023, Geochemistry of the Turonian-Coniacian strata: New insight into paleoenvironmental conditions of the Tethys, Eastern Pontides, NE Türkiye: Journal of Asian Earth Sciences, v. 10, p. 100156. doi: 10.1016/j.jaesx.2023.100156

Özyurt, M, and Kırmacı, M.Z., 2024, Microfacies and geochemistry of Kimmeridgian limestone strata in the Eastern Pontides (North-East Turkey): Palaeoclimate and palaeoenvironmental influence on organic matter enrichment: The Depositional Record, doi: 10.1002/dep2.286

Özyurt, M., Kırmacı, M.Z., and Al-Aasm, I.S., 2019b, Geochemical characteristics of Upper Jurassic–Lower Cretaceous platform carbonates in Hazine Mağara, Gümüşhane (northeast Turkey): Implications for dolomitization and recrystallization: Canadian Journal of Earth Sciences, v. 56, no. 3, p. 306–320. doi: 10.1139/cjes-2018-0168

Özyurt, M., Kırmacı, M.Z., Al-Aasm, I., Hollis, C., Taslı, K., and Kandemir, R., 2020, REE characteristics of lower cretaceous limestone succession in gümüşhane, NE Turkey: Implications for ocean paleoredox conditions and diagenetic alteration: Minerals, v. 10, no. 8, p. 683

Özyurt, M., Kırmacı, M.Z., Al-Aasm, I.S., and Kandemir, R., 2024, Geochemistry of the massive dolomites in Eastern Black Sea Region: REE implications for dolomite petrogenesis: Journal of Geochemistry International, v. 62, no. 2, p. 184–207.

Özyurt, M., Kırmacı, M.Z., Yılmaz, İ.Ö., Kandemir, R., and Taslı, K., 2022, Sedimentological and geochemical approaches for determination of the palaeoceanographic and palaeoclimatic conditions of Lower Cretaceous marine deposits in the eastern part of Sakarya Zone, NE Turkey: Carbonates and Evaporites, v. 37, no. 2, p. 25. doi: 10.1007/s13146-022-00768-3

Özyurt, M., Ziya Kirmaci, M., Ömer Yılmaz, İ., and Kandemir, R., 2019c. Sedimentological and Geochemical Records of Lower Cretaceous Carbonate Successions Around Trabzon (NE Turkey): Implications for Paleoenvironmental Evolution and Paleoclimatological Conditions of Tethys. In Patterns and Mechanisms of Climate, Paleoclimate and Paleoenvironmental Changes from Low-Latitude Regions: Proceedings of the 1st Springer Conference of the Arabian Journal of Geosciences (CAJG-1), Tunisia, 2018: Springer International Publishing, p. 19–21.

Palma, R.M., and Angeleri, M.A., 1992, Early Cretaceous serpulid limestones: Chachao Formation, Neuquen Basin, Argentina: Facies, v. 27, p. 175–178

Palmer, T.J., and Wilson, M.A., 1990, Growth of ferruginous oncoliths in the Bajocian (Middle Jurassic) of Europe: Terra Nova, v. 2, p. 142–147, no. 2. doi: 10.1111/j.1365-3121.1990.tb00055.x

Pelin, S., 1977, Geological study of the area southeast of Alucra (Giresun) with special reference to its petroleum potential. Karadeniz teknik universitesi, yerbilimleri dergisi: Jeoloji, v. 1, p. 15–20

Pérez, M.R., and Nieto, L.M., 2010, Jurassic Fe-Mn macro-oncoids from pelagic swells of the External Subbetic (Spain): Evidences of microbial origin: Geologica Acta, v. 8, no. 2, p. 151–168

Pomoni-Papaioannou, F., 1994, Palaeoenvironmental reconstruction of a condensed hardground-type depositional sequence at the Cretaceous-Tertiary contact in the Parnassus-Ghiona zone, central Greece: Sedimentary Geology, v. 93, no. 1–2, p. 7–24. doi: 10.1016/0037-0738(94)90026-4

Preat, A.R., De Jong, J.T., De Ridder, C., and Gillan, D.C., 2011, Possible Fe isotope fractionation during microbiological processing in ancient and modern marine environments: STROMATOLITES: Interaction of Microbes with Sediments, Cellular Origin, Life in Extreme Habitats and Astrobiology, v. 18 , p. 651–673. doi: 10.1007/978-94-007-0397-1_29

Preat, A., Mamet, B., De Ridder, C., Boulvain, F., and Gillan, D., 2000, Iron bacterial and fungal mats, Bajocian stratotype (Mid-Jurassic, northern Normandy, France): Sedimentary Geology, v. 137, no. 3–4, p. 107–126. doi: 10.1016/S0037-0738(00)00101-9

Preat, A., Préat, A., Hantzpergue, P., and Mamet, B., 2006, Origin and evolution of microstromatolites following postdepositional processes: A 2.2 Ga-old example from the Kona dolomite (Transvaal Supergroup, South Africa): Journal of Sedimentary Research, v. 76, no. 11–12, p. 1376–1388

Preto, N., Breda, A., Corso, J.D., Franceschi, M., Rocca, F., Spada, C., and Roghi, G., 2017, The Loppio Oolitic Limestone (Early Jurassic, Southern Alps): A prograding oolitic body with high original porosity originated by a carbonate platform crisis and recovery: Marine and Petroleum Geology, v. 79, p. 394–411. doi: 10.1016/j.marpetgeo.2016.10.027

Reolid, M., 2011, Palaeoenvironmental contexts for microbial commu nities from Fe-Mn crusts of middle-upper Jurassic hardgrounds (Betic-Rifan Cordillera): Revista espanola de paleontologia, v. 26, p. 135–160, no. 2. doi: 10.7203/sjp.26.2.18537

Reolid, M., and Abad, I., 2019, Jurassic non-carbonate microbialites from the Betic-Rifian Cordillera (Tethys western end): Textures, mineralogy, and environmental reconstruction: Minerals, v. 9, no. 2, p. 88. doi: 10.3390/min9020088

Reolid, M., Chakiri, S., and Bejjaji, Z., 2013, Adaptative strategies of the Toarcian benthic foraminiferal assemblages from the Middle Atlas (Morocco): Palaeoecological implications: Journal of African Earth Sciences, v. 84, p. 1–12. doi: 10.1016/j.jafrearsci.2013.03.008

Reolid, M., Gaillard, C., Olóriz, F., and Rodríguez-Tovar, F.J., 2005, Microbial encrustations from the Middle Oxfordian-earliest Kimmeridgian lithofacies in the prebetic zone (Betic Cordillera, southern Spain): Characterization, distribution and controlling factors, Facies, v. 50, p. 529–543.

Reolid, M., and Martínez-Ruiz, F., 2012, Comparison of benthic foraminifera and geochemical proxies in shelf deposits from the Upper Jurassic of the Prebetic (southern Spain): Journal

of Iberian Geology, v. 38, no. 2, p. 449–465. doi: 10.5209/rev_JIGE.2012.v38.n2.40468
Reolid, M., and Molina, J.M., 2010, Serpulid-Frutexites assemblage from shadow-cryptic environments in Jurassic Marine Caves betic Cordillera, Southern spain: Palaios, v. 25, no. 7, p. 468–474. doi: 10.2110/palo.2009.p09-150r
Reolid, M., and Nieto, L.M., 2010, Microbial induced sedimentary structures in Jurassic "ammonitico rosso" from the Betic Cordillera (SE Spain): Importance for the fossil record: Facies, v. 56, no. 2, p. 275–292
Robertson, A.H.F., and Dixon, J.E., 1984, Introduction: Aspects of the geological evolution of the Eastern Mediterranean: Geological Society, London, Special Publications, v. 17, no. 1, p. 1–74. doi: 10.1144/GSL.SP.1984.017.01.02
Robinson, A.G., Banks, C.J., Rutherford, M.M., and Hirst, J.P.P., 1995, Stratigraphic and structural development of the Eastern Pontides, Turkey: Journal of the Geological Society, v. 152, no. 5, p. 861–872. doi: 10.1144/gsjgs.152.5.0861
Rojkovič, I., Aubrecht, R., and Mišík, M., 2003, Mineral and chemical com position of manganese hardgrounds in Jurassic limestones of the Western Carpathians: Geologica Carpathica, v. 54, p. 317–328
Salama, W., El Aref, M.M., and Gaupp, R., 2013, Mineral evolution and processes of ferruginous microbialite accretion–an example from the M iddle E ocene stromatolitic and ooidal ironstones of the B ahariya D epression, W estern D esert, E gypt: Geobiology, v. 11, no. 1, p. 15–28. doi: 10.1111/gbi.12011
Santantonio, M., 1993, Facies associations and evolution of pelagic carbonate platform/basin systems: Examples from the Italian Jurassic: Sedimentology, v. 40, no. 6, p. 1039–1067. doi: 10.1111/j.1365-3091.1993.tb01379.x
Schieber, J., 1999, Microbial mats in terrigenous clastics; the challenge of identification in the rock record: Palaios, v. 14, p. 3–12, no. 1. doi: 10.2307/3515357
Scopellito, G., and Rusco, V., 2021, Petrographic and geochemical characterization of the Middle–Upper Jurassic Fe–Mn crusts and mineralizations from Monte Inici (north-western Sicily): Genetic implications: International Journal of Earth Sciences, v. 110, p. 559–582, no. 2. doi: 10.1007/s00531-020-01971-0
Scotese, C.R., 2021, An atlas of phanerozoic paleogeographic maps: The seas come in and the seas go out: Annual Review of Earth and Planetary Sciences, v. 49, p. 679–728.
Şen, C., 2007, Jurassic volcanism in the Eastern Pontides: Is it rift related or subduction related?: Turkish Journal of Earth Sciences, v. 16, no. 4, p. 523–539
Şengör, A.M.C., 1979, The North Anatolian transform fault: Its age, offset and tectonic significance: Journal of the Geological Society, v. 136, no. 3, p. 269–282. doi: 10.1144/gsjgs.136.3.0269
Şengör, A.C., Altıner, D., Zabcı, C., Sunal, G., Lom, N., Aylan, E., and Öner, T., 2023, On the nature of the Cimmerian Continent: Earth-Science Reviews, v. 104520, p. 104520. doi: 10.1016/j.earscirev.2023.104520
Şengör, A.C., and Yilmaz, Y., 1981, Tethyan evolution of Turkey: A plate tectonic approach: Tectonophysics, v. 75, no. 3–4, p. 181–241. doi: 10.1016/0040-1951(81)90275-4
Şengör, A.C., Yilmaz, Y., and Ketin, I., 1980, Remnants of a pre–Late Jurassic ocean in northern Turkey: Fragments of Permian-Triassic Paleo-Tethys?: Geological Society of America Bulletin, v. 91, no. 10, p. 599–609. doi: 10.1130/0016-7606(1980)91<599:ROAPJO>2.0.CO;2
Şengör, A.C., Yılmaz, Y., and Sungurlu, O., 1984, Tectonics of the Mediterranean Cimmerides: nature and evolution of the western termination of Palaeo-Tethys: Geological Society, London, Special Publications, v. 17, no. 1, p. 77–112.
Sequero, C., Aurell, M., and Bádenas, B., 2020, Oncoid distribution in the shallow domains of a Kimmeridgian carbonate ramp (Late Jurassic, NE Spain): Sedimentary Geology, v. 398, p. 105585. doi: 10.1016/j.sedgeo.2019.105585
Shields, G., and Stille, P., 2001, Diagenetic constraints on the use of cerium anomalies as palaeoseawater redox proxies: An isotopic and REE study of Cambrian phosphorites: Chemical Geology, v. 175, no. 1–2, p. 29–48.
Šmuc, A., and Rožič, B., 2010, The Jurassic Prehodavci Formation of the Julian Alps: Easternmost outcrops of Rosso Ammonitico in the Southern Alps (NW Slovenia): Swiss Journal of Geosciences, v. 103, p. 241–255, no. 2. doi: 10.1007/s00015-010-0015-3
Sturesson, U., Heikoop, J.M., and Risk, M.J., 2000, Modern and Palaeozoic iron ooids—a similar volcanic origin: Sedimentary Geology, v. 136, no. 1–2, p. 137–146.
Taylor, S.R., and McLennan, S.M. 1985, The Continental Crust: Its Composition and Evolution: Blackwell, Oxford Press, p. 1–312.
Todd, S.E., Pufahl, P.K., Murphy, J.B., and Taylor, K.G., 2019, Sedimentology and oceanography of early Ordovician ironstone, Bell Island, Newfoundland: Ferruginous seawater and upwelling in the Rheic Ocean: Sedimentary Geology, v. 379, p. 1–15.
Topuz, G., Altherr, R., Satır, M., and Schwarz, W.H., 2004, Low-grade metamorphic rocks from the Pulur complex, NE Turkey: Implications for the pre-Liassic evolution of the Eastern Pontides: International Journal of Earth Sciences, v. 93, p. 72–91, no. 1. doi: 10.1007/s00531-003-0372-5
Topuz, G., Altherr, R., Siebel, W., Schwarz, W.H., Zack, T., and Hasözbek, A. . . ., and Barth, M., Satır, M., Şen, C., 2010, Carboniferous high-potassium I-type granitoid magmatism in the Eastern Pontides: The Gümüşhane pluton (NE Turkey): Lithos, v. 116, no. 1–2, p. 92–110. doi: 10.1016/j.lithos.2010.01.003
Toth, J.R., 1980, Deposition of submarine crusts rich in manganese and iron, Bulletin of the Geological Society of America, v. 91, p. 44–54, no. 1. doi: 10.1130/0016-7606(1980)91<44:DOSCRI>2.0.CO;2
Tucker, M.E., and Wright, V.P., 1990, Carbonate Sedimentology, John Wiley & Sons.
Tyszka, J., and Kaminski, M.A. (1995). Factors controlling the distribution of agglutinated foraminifera in Aalenian–Bajocian dysoxic facies (Pieniny Klippen Belt, Poland). *In* Proceedings of the Fourth International Workshop on Agglu– tinated Foraminifera (Grzybowski Foundation Special Publication), vol. 3, p. 271–291.
Usui, A., Bau, M., and Toshitsugu, Y., 1997, Manganese microchimneys buried in the Central Pacific pelagic sediments: Evidence of intraplate water circulation?: Marine Geology, v. 141, no. 1–4, p. 269–285. doi: 10.1016/S0025-3227(97)00070-4
Vera, J.A., and Martín-Algarra, A., 2012, Mesozoic stratigraphic breaks and pelagic stromatolites in the Betic Cordillera, Southern Spain, *in* Bertrand-Sarfati, J., and Monty, C., eds. Phanerozoic stromatolites II: Dordrecht, Springer Science & Business Media, pp. 319–344.

Vörös, A., and Kandemir, R., 2011, A new Early Jurassic brachiopod fauna from the Eastern Pontides (Turkey): Neues Jahrbuch Fur Geologie Und Palaontologie-Abhandlungen, v. 260, no. 3, p. 343. doi: 10.1127/0077-7749/2011/0146

Xiao, E.Z., Mei, M.X., Jiang, S., and Zafar, T., 2020, Morphology and features of Cambrian oncoids and responses to palaeogeography of the North China Platform: Journal of Palaeogeography, v. 9, p. 1–18, no. 1. doi: 10.1186/s42501-020-0055-1

Yilmaz, C., and Kandemir, R.A.I.F., 2006, Sedimentary records of the extensional tectonic regime with temporal cessation: Gumushane Mesozoic Basin (NE Turkey): Geologica Carpathica-Bratislava, v. 57, no. 1, p. 3

Yılmaz, Y., Tüysüz, O., Yiğitbaş, E., Genç, Ş.C., and Şengör, A.M.C., 1997, Geology and tectonic evolution of the Pontides: Regional and Petroleum Geology of the Black Sea and Surrounding Region, v. 68, p. 183–226

Zafar, T., Frontalini, F., Rehman, H.U., Khan, D., Ullah, Z., and Ur Rahim, H., Oyebamiji, A., Hussain, Z., Song, S., Farhan, M., Ahmed, M.S., Sami, M., and Fathy, D., 2024, Understanding the origin of Cambrian marine oncoids: A petrologic, geochemical, and isotopic perspective: Sedimentary Geology, v. 466, p. 106638. doi: 10.1016/j.sedgeo.2024.106638

Zang, W.L., Reuning, L., and Yuan, D.X., 2015, Microbial-mediated mineralization in modern and ancient environments: New insights into an old controversial theme: Earth-Science Reviews, v. 150, p. 1–20

Zatoń, M., Kremer, B., Marynowski, L., Wilson, M.A., and Krawczyński, W., 2012, Middle Jurassic (Bathonian) encrusted oncoids from the Polish Jura, southern Poland: Facies, v. 58, p. 57–77, no. 1. doi: 10.1007/s10347-011-0273-1